

Fine-mapping of 150 breast cancer risk regions identifies 178 high confidence target genes

Laura Fachal¹, Hugues Aschard^{2-4,275}, Jonathan Beesley^{5,275}, Daniel R. Barnes⁶, Jamie Allen⁶, Siddhartha Kar¹, Karen A. Pooley⁶, Joe Dennis⁶, Kyriaki Michailidou^{6, 7}, Constance Turman⁴, Penny Soucy⁸, Audrey Lemaçon⁸, Michael Lush⁶, Jonathan P. Tyrer¹, Maya Ghoussaini¹, Mahdi Moradi Marjaneh⁵, Xia Jiang³, Simona Agata⁹, Kristiina Aittomäki¹⁰, M. Rosario Alonso¹¹, Irene L. Andrulis^{12, 13}, Hoda Anton-Culver¹⁴, Natalia N. Antonenkova¹⁵, Adalgeir Arason^{16, 17}, Volker Arndt¹⁸, Kristan J. Aronson¹⁹, Banu K. Arun²⁰, Bernd Auber²¹, Paul L. Auer^{22, 23}, Jacopo Azzollini²⁴, Judith Balmaña²⁵, Rosa B. Barkardottir^{16, 17}, Daniel Barrowdale⁶, Alicia Beeghly-Fadiel²⁶, Javier Benitez^{27, 28}, Marina Bermisheva²⁹, Katarzyna Białkowska³⁰, Amie M. Blanco³¹, Carl Blomqvist^{32, 33}, William Blot^{26, 34}, Natalia V. Bogdanova^{15, 35, 36}, Stig E. Bojesen³⁷⁻³⁹, Manjeet K. Bolla⁶, Bernardo Bonanni⁴⁰, Ake Borg⁴¹, Kristin Bosse⁴², Hiltrud Brauch⁴³⁻⁴⁵, Hermann Brenner^{18, 45, 46}, Ignacio Briceno^{47, 48}, Ian W. Brock⁴⁹, Angela Brooks-Wilson^{50, 51}, Thomas Brüning⁵², Barbara Burwinkel^{53, 54}, Sandra S. Buys⁵⁵, Qiuyin Cai²⁶, Trinidad Caldés⁵⁶, Maria A. Caligo⁵⁷, Nicola J. Camp⁵⁸, Ian Campbell^{59, 60}, Federico Canzian⁶¹, Jason S. Carroll⁶², Brian D. Carter⁶³, Jose E. Castela⁶⁴, Jocelyne Chiquette⁶⁵, Hans Christiansen³⁵, Wendy K. Chung⁶⁶, Kathleen B.M. Claes⁶⁷, Christine L. Clarke⁶⁸, GEMO Study Collaborators⁶⁹⁻⁷¹, EMBRACE Collaborators⁶, J. Margriet Collée⁷², Sten Cornelissen⁷³, Fergus J. Couch⁷⁴, Angela Cox⁴⁹, Simon S. Cross⁷⁵, Cezary Cybulski³⁰, Kamila Czene⁷⁶, Mary B. Daly⁷⁷, Miguel de la Hoya⁵⁶, Peter Devilee^{78, 79}, Orland Diez^{25, 80}, Yuan Chun Ding⁸¹, Gillian S. Dite⁸², Susan M. Domchek⁸³, Thilo Dörk³⁶, Isabel dos-Santos-Silva⁸⁴, Arnaud Droit^{8, 85}, Stéphane Dubois⁸, Martine Dumont⁸⁶, Mercedes Duran⁸⁷, Lorraine Durcan^{88, 89}, Miriam Dwek⁹⁰, Diana M. Eccles⁸⁹, Christoph Engel^{91, 92}, Mikael Eriksson⁷⁶, D. Gareth Evans^{93, 94}, Peter A. Fasching^{95, 96}, Olivia Fletcher⁹⁷, Giuseppe Floris⁹⁸, Henrik Flyger⁹⁹, Lenka Foretova¹⁰⁰, William D. Foulkes¹⁰¹, Eitan Friedman^{102, 103}, Lin

Fritsch¹⁰⁴, Debra Frost⁶, Marike Gabrielson⁷⁶, Manuela Gago-Dominguez^{105, 106}, Gaetana Gambino¹⁰⁷, Patricia A. Ganz¹⁰⁸, Susan M. Gapstur⁶³, Judy Garber¹⁰⁹, José A. García-Sáenz⁵⁶, Mia M. Gaudet⁶³, Vassilios Georgoulas¹¹⁰, Graham G. Giles^{82, 111, 112}, Gord Glendon¹², Andrew K. Godwin¹¹³, Mark S. Goldberg^{114, 115}, David E. Goldgar¹¹⁶, Anna González-Neira²⁸, Mark H. Greene¹¹⁷, Mervi Grip¹¹⁸, Jacek Gronwald³⁰, Anne Grundy¹¹⁹, Pascal Guénel¹²⁰, Eric Hahnen^{121, 122}, Christopher A. Haiman¹²³, Niclas Håkansson¹²⁴, Per Hall^{76, 125}, Ute Hamann¹²⁶, Patricia A. Harrington¹, Jaana M. Hartikainen¹²⁷⁻¹²⁹, Mikael Hartman^{130, 131}, Wei He⁷⁶, Catherine S. Healey¹, Bernadette A.M. Heemskerk-Gerritsen¹³², Jane Heyworth¹³³, Peter Hillemanns³⁶, Frans B.L. Hogervorst¹³⁴, Antoinette Hollestelle¹³², Maartje J. Hoening¹³², John L. Hopper⁸², Anthony Howell¹³⁵, Guanmengqian Huang¹²⁶, Peter J. Hulick^{136, 137}, Evgeny N. Imyanitov¹³⁸, ABCTB Investigators¹³⁹, KConFab Investigators^{59, 60}, HEBON Investigators¹⁴⁰, Claudine Isaacs¹⁴¹, Motoki Iwasaki¹⁴², Agnes Jager¹³², Milena Jakimovska¹⁴³, Anna Jakubowska^{30, 144}, Paul James^{60, 145}, Ramunas Janavicius¹⁴⁶, Rachel C. Jankowitz¹⁴⁷, Esther M. John¹⁴⁸, Nichola Johnson⁹⁷, Michael E. Jones¹⁴⁹, Arja Jukkola-Vuorinen¹⁵⁰, Audrey Jung¹⁵¹, Rudolf Kaaks¹⁵¹, Daehee Kang¹⁵²⁻¹⁵⁴, Beth Y. Karlan¹⁵⁵, Renske Keeman⁷³, Michael J. Kerin¹⁵⁶, Elza Khusnutdinova^{29, 157}, Johanna I. Kiiski¹⁵⁸, Judy Kirk¹⁵⁹, Cari M. Kitahara¹⁶⁰, Yon-Dschun Ko¹⁶¹, Irene Konstantopoulou¹⁶², Veli-Matti Kosma¹²⁷⁻¹²⁹, Stella Koutros¹⁶³, Katerina Kubelka-Sabit¹⁶⁴, Ava Kwong¹⁶⁵⁻¹⁶⁷, Kyriacos Kyriacou⁷, Yael Laitman¹⁰², Diether Lambrechts^{168, 169}, Eunjung Lee¹²³, Goska Leslie⁶, Jenny Lester¹⁵⁵, Fabienne Lesueur^{70, 71, 170}, Annika Lindblom^{171, 172}, Wing-Yee Lo^{43, 44}, Jirong Long²⁶, Artitaya Lophatananon^{173, 174}, Jennifer T. Loud¹¹⁷, Jan Lubiński³⁰, Robert J. MacInnis^{82, 111}, Tom Maishman^{88, 89}, Enes Makalic⁸², Arto Mannermaa¹²⁷⁻¹²⁹, Mehdi Manoochehri¹²⁶, Siranoush Manoukian²⁴, Sara Margolin^{125, 175}, Maria Elena Martinez^{106, 176}, Keitaro Matsuo^{177, 178}, Tabea Maurer¹⁷⁹, Dimitrios Mavroudis¹¹⁰, Rebecca Mayes¹, Lesley McGuffog⁶, Catriona McLean¹⁸⁰, Noura Mebirouk⁶⁹⁻⁷¹, Alfons Meindl¹⁸¹, Pooja Middha^{151, 182}, Nicola Miller¹⁵⁶, Austin Miller¹⁸³,

Marco Montagna⁹, Fernando Moreno⁵⁶, Anna Marie Mulligan^{184, 185}, Victor M. Muñoz-Garzon¹⁸⁶, Taru A. Muranen¹⁵⁸, Steven A. Narod¹⁸⁷, Rami Nassir¹⁸⁸, Katherine L. Nathanson⁸³, Susan L. Neuhausen⁸¹, Heli Nevanlinna¹⁵⁸, Patrick Neven⁹⁸, Finn C. Nielsen¹⁸⁹, Liene Nikitina-Zake¹⁹⁰, Aaron Norman¹⁹¹, Kenneth Offit^{192, 193}, Edith Olah¹⁹⁴, Olufunmilayo I. Olopade¹⁹⁵, Håkan Olsson¹⁹⁶, Nick Orr¹⁹⁷, Ana Osorio^{27, 28}, V. Shane Pankratz¹⁹⁸, Janos Papp¹⁹⁴, Sue K. Park¹⁵²⁻¹⁵⁴, Tjoung-Won Park-Simon³⁶, Michael T. Parsons⁵, James Paul¹⁹⁹, Inge Sokilde Pedersen²⁰⁰, Bernard Peissel²⁴, Beth Peshkin¹⁴¹, Paolo Peterlongo²⁰¹, Julian Peto⁸⁴, Dijana Plaseska-Karanfilska¹⁴³, Karolina Prajzendanz³⁰, Ross Prentice²², Nadege Presneau⁹⁰, Darya Prokofyeva¹⁵⁷, Miquel Angel Pujana²⁰², Katri Pylkäs^{203, 204}, Paolo Radice²⁰⁵, Susan J. Ramus^{206, 207}, Johanna Rantala²⁰⁸, Rohini Rau-Murthy¹⁹³, Gad Rennert²⁰⁹, Harvey A. Risch²¹⁰, Mark Robson¹⁹³, Atocha Romero²¹¹, Caroline Maria Rossing¹⁸⁹, Emmanouil Saloustros²¹², Estela Sánchez-Herrero²¹¹, Dale P. Sandler²¹³, Marta Santamariña^{27, 214, 215}, Christobel Saunders²¹⁶, Elinor J. Sawyer²¹⁷, Maren T. Scheuner³¹, Daniel F. Schmidt^{82, 218}, Rita K. Schmutzler^{121, 122}, Andreas Schneeweiss^{54, 219}, Minouk J. Schoemaker¹⁴⁹, Ben Schöttker^{18, 220}, Peter Schürmann³⁶, Christopher Scott¹⁹¹, Rodney J. Scott²²¹⁻²²³, Leigha Senter²²⁴, Caroline MD Seynaeve¹³², Mitul Shah¹, Priyanka Sharma²²⁵, Chen-Yang Shen^{226, 227}, Xiao-Ou Shu²⁶, Christian F. Singer²²⁸, Thomas P. Slavin²²⁹, Snezhana Smichkoska²³⁰, Melissa C. Southey^{86, 231}, John J. Spinelli^{232, 233}, Amanda B. Spurdle⁵, Jennifer Stone^{82, 234}, Dominique Stoppa-Lyonnet^{69, 235, 236}, Christian Sutter²³⁷, Anthony J. Swerdlow^{149, 238}, Rulla M. Tamimi^{3, 4, 239}, Yen Yen Tan²⁴⁰, William J. Tapper²⁴¹, Jack A. Taylor^{213, 242}, Manuel R. Teixeira^{243, 244}, Maria Tengström^{127, 245, 246}, Soo H. Teo^{247, 248}, Mary Beth Terry²⁴⁹, Alex Teulé²⁵⁰, Mads Thomassen²⁵¹, Darcy L. Thull²⁵², Maria Grazia Tibiletti²⁵³, Marc Tischkowitz^{101, 254}, Amanda E. Toland²⁵⁵, Rob A.E.M. Tollenaar²⁵⁶, Ian Tomlinson^{257, 258}, Diana Torres^{47, 126}, Gabriela Torres-Mejía²⁵⁹, Melissa A. Troester²⁶⁰, Nadine Tung²⁶¹, Maria Tzardi²⁶², Hans-Ulrich Ulmer²⁶³, Celine M. Vachon²⁶⁴, Christi J. van Asperen²⁶⁵, Lizet E. van der Kolk¹³⁴, Elizabeth J. van

Rensburg²⁶⁶, Ana Vega^{27, 214, 215}, Alessandra Viel²⁶⁷, Joseph Vijai^{192, 193}, Maatje J. Vogel²⁶⁸, Qin Wang⁶, Barbara Wappenschmidt^{121, 122}, Clarice R. Weinberg²⁶⁹, Jeffrey N. Weitzel²²⁹, Camilla Wendt¹⁷⁵, Hans Wildiers⁹⁸, Robert Winqvist^{203, 204}, Alicja Wolk^{124, 270}, Anna H. Wu¹²³, Drakoulis Yannoukakos¹⁶², Yan Zhang^{18, 45}, Wei Zheng²⁶, Paul D.P. Pharoah^{1, 6}, Jenny Chang-Claude^{151, 179}, Montserrat García-Closas^{163, 271}, Marjanka K. Schmidt^{73, 272}, Roger L. Milne^{82, 86, 111}, Vessela N. Kristensen^{273, 274}, Juliet D. French⁵, Stacey L. Edwards⁵, Antonis C. Antoniou⁶, Georgia Chenevix-Trench^{5,276}, Jacques Simard^{8,276}, Douglas F. Easton^{1, 6,276}, Peter Kraft^{3, 4,276,*}, Alison M. Dunning^{1,276,*}

¹ Centre for Cancer Genetic Epidemiology, Department of Oncology, University of Cambridge, Cambridge, CB1 8RN, UK.

² Centre de Bioinformatique, Biostatistique et Biologie Intégrative (C3BI), Institut Pasteur, Paris, France.

³ Program in Genetic Epidemiology and Statistical Genetics, Harvard T.H. Chan School of Public Health, Boston, MA, 02115, USA.

⁴ Department of Epidemiology, Harvard T.H. Chan School of Public Health, Boston, MA, 02115, USA.

⁵ Department of Genetics and Computational Biology, QIMR Berghofer Medical Research Institute, Brisbane, Queensland, 4006, Australia.

⁶ Centre for Cancer Genetic Epidemiology, Department of Public Health and Primary Care, University of Cambridge, Cambridge, CB1 8RN, UK.

⁷ Department of Electron Microscopy/Molecular Pathology and The Cyprus School of Molecular Medicine, The Cyprus Institute of Neurology & Genetics, Nicosia, 1683, Cyprus.

⁸ Genomics Center, Centre Hospitalier Universitaire de Québec – Université Laval, Research Center, Québec City, QC, G1V 4G2, Canada.

⁹ Immunology and Molecular Oncology Unit, Veneto Institute of Oncology IOV - IRCCS, Padua, 35128, Italy.

¹⁰ Department of Clinical Genetics, Helsinki University Hospital, University of Helsinki, Helsinki, 00290, Finland.

¹¹ Human Genotyping-CEGEN Unit, Human Cancer Genetic Program, Spanish National Cancer Research Centre, Madrid, 28029, Spain.

¹² Fred A. Litwin Center for Cancer Genetics, Lunenfeld-Tanenbaum Research Institute of Mount Sinai Hospital, Toronto, ON, M5G 1X5, Canada.

¹³ Department of Molecular Genetics, University of Toronto, Toronto, ON, M5S 1A8, Canada.

¹⁴ Department of Epidemiology, Genetic Epidemiology Research Institute, University of California Irvine, Irvine, CA, 92617, USA.

¹⁵ N.N. Alexandrov Research Institute of Oncology and Medical Radiology, Minsk, 223040, Belarus.

¹⁶ Department of Pathology, Landspítali University Hospital, Reykjavik, 101, Iceland.

¹⁷ BMC (Biomedical Centre), Faculty of Medicine, University of Iceland, Reykjavik, 101, Iceland.

¹⁸ Division of Clinical Epidemiology and Aging Research, C070, German Cancer Research Center (DKFZ), Heidelberg, 69120, Germany.

¹⁹ Department of Public Health Sciences, and Cancer Research Institute, Queen's University, Kingston, ON, K7L 3N6, Canada.

²⁰ Department of Breast Medical Oncology, University of Texas MD Anderson Cancer Center, Houston, TX, 77030, USA.

²¹ Institute of Human Genetics, Hannover Medical School, Hannover, 30625, Germany.

²² Cancer Prevention Program, Fred Hutchinson Cancer Research Center, Seattle, WA, 98109, USA.

- ²³ Zilber School of Public Health, University of Wisconsin-Milwaukee, Milwaukee, WI, 53205, USA.
- ²⁴ Unit of Medical Genetics, Department of Medical Oncology and Hematology, Fondazione IRCCS (Istituto di Ricovero e Cura a Carattere Scientifico) Istituto Nazionale dei Tumori di Milano, Milan, 20133, Italy.
- ²⁵ High Risk and Cancer Prevention Group, Vall d'Hebron Institute of Oncology, Barcelona, 08035, Spain.
- ²⁶ Division of Epidemiology, Department of Medicine, Vanderbilt Epidemiology Center, Vanderbilt-Ingram Cancer Center, Vanderbilt University School of Medicine, Nashville, TN, 37232, USA.
- ²⁷ Centro de Investigación en Red de Enfermedades Raras (CIBERER), Valencia, 46010, Spain.
- ²⁸ Human Cancer Genetics Programme, Spanish National Cancer Research Centre (CNIO), Madrid, 28029, Spain.
- ²⁹ Institute of Biochemistry and Genetics, Ufa Scientific Center of Russian Academy of Sciences, Ufa, 450054, Russia.
- ³⁰ Department of Genetics and Pathology, Pomeranian Medical University, Szczecin, 71-252, Poland.
- ³¹ Cancer Genetics and Prevention Program, University of California San Francisco, San Francisco, CA, 94143-1714, USA.
- ³² Department of Oncology, Helsinki University Hospital, University of Helsinki, Helsinki, 00290, Finland.
- ³³ Department of Oncology, Örebro University Hospital, Örebro, 70185, Sweden.
- ³⁴ International Epidemiology Institute, Rockville, MD, 20850, USA.
- ³⁵ Department of Radiation Oncology, Hannover Medical School, Hannover, 30625, Germany.
- ³⁶ Gynaecology Research Unit, Hannover Medical School, Hannover, 30625, Germany.
- ³⁷ Copenhagen General Population Study, Herlev and Gentofte Hospital, Copenhagen University Hospital, Herlev, 2730, Denmark.

³⁸ Department of Clinical Biochemistry, Herlev and Gentofte Hospital, Copenhagen University Hospital, Herlev, 2730, Denmark.

³⁹ Faculty of Health and Medical Sciences, University of Copenhagen, Copenhagen, 2200, Denmark.

⁴⁰ Division of Cancer Prevention and Genetics, IEO, European Institute of Oncology IRCCS, Milan, 20141, Italy.

⁴¹ Department of Oncology, Lund University and Skåne University Hospital, Lund, 222 41, Sweden.

⁴² Institute of Medical Genetics and Applied Genomics, University of Tübingen, Tübingen, 72074, Germany.

⁴³ Dr. Margarete Fischer-Bosch-Institute of Clinical Pharmacology, Stuttgart, 70376, Germany.

⁴⁴ University of Tübingen, Tübingen, 72074, Germany.

⁴⁵ German Cancer Consortium (DKTK), German Cancer Research Center (DKFZ), Heidelberg, 69120, Germany.

⁴⁶ Division of Preventive Oncology, German Cancer Research Center (DKFZ) and National Center for Tumor Diseases (NCT), Heidelberg, 69120, Germany.

⁴⁷ Institute of Human Genetics, Pontificia Universidad Javeriana, Bogota, Colombia.

⁴⁸ Medical Faculty, Universidad de La Sabana, Bogota, Colombia.

⁴⁹ Sheffield Institute for Nucleic Acids (SInFoNiA), Department of Oncology and Metabolism, University of Sheffield, Sheffield, S10 2TN, UK.

⁵⁰ Genome Sciences Centre, BC Cancer Agency, Vancouver, BC, V5Z 1L3, Canada.

⁵¹ Department of Biomedical Physiology and Kinesiology, Simon Fraser University, Burnaby, BC, V5A 1S6, Canada.

⁵² Institute for Prevention and Occupational Medicine of the German Social Accident Insurance, Institute of the Ruhr University Bochum (IPA), Bochum, 44789, Germany.

⁵³ Molecular Epidemiology Group, C080, German Cancer Research Center (DKFZ), Heidelberg, 69120, Germany.

⁵⁴ Molecular Biology of Breast Cancer, University Womens Clinic Heidelberg, University of Heidelberg, Heidelberg, 69120, Germany.

⁵⁵ Department of Medicine, Huntsman Cancer Institute, Salt Lake City, UT, 84112, USA.

⁵⁶ Medical Oncology Department, Hospital Clínico San Carlos, Instituto de Investigación Sanitaria San Carlos (IdISSC), Centro Investigación Biomédica en Red de Cáncer (CIBERONC), Madrid, 28040, Spain.

⁵⁷ Section of Molecular Genetics, Dept. of Laboratory Medicine, University Hospital of Pisa, Pisa, Italy.

⁵⁸ Department of Internal Medicine, Huntsman Cancer Institute, Salt Lake City, UT, 84112, USA.

⁵⁹ Research Department, Peter MacCallum Cancer Center, Melbourne, Victoria, 3000, Australia.

⁶⁰ Sir Peter MacCallum Department of Oncology, The University of Melbourne, Melbourne, Victoria, 3000, Australia.

⁶¹ Genomic Epidemiology Group, German Cancer Research Center (DKFZ), Heidelberg, 69120, Germany.

⁶² Cancer Research UK Cambridge Research Institute, Li Ka Shing Centre, University of Cambridge, Cambridge, UK.

⁶³ Epidemiology Research Program, American Cancer Society, Atlanta, GA, 30303, USA.

⁶⁴ Oncology and Genetics Unit, Instituto de Investigación Sanitaria Galicia Sur (IISGS), Xerencia de Xestión Integrada de Vigo-SERGAS, Vigo, 36312, Spain.

⁶⁵ CRCHU de Québec-oncologie, Québec, QC, G1S 4L8, Canada.

⁶⁶ Departments of Pediatrics and Medicine, Columbia University, New York, NY, 10032, USA.

⁶⁷ Centre for Medical Genetics, Ghent University, Gent, 9000, Belgium.

⁶⁸ Westmead Institute for Medical Research, University of Sydney, Sydney, New South Wales, 2145, Australia.

⁶⁹ Department of Tumour Biology, INSERM U830, Paris, 75005, France.

⁷⁰ Institut Curie, Paris, 75005, France.

⁷¹ Mines ParisTech, Fontainebleau, 77305, France.

⁷² Department of Clinical Genetics, Erasmus University Medical Center, Rotterdam, 3015 CN, The Netherlands.

⁷³ Division of Molecular Pathology, The Netherlands Cancer Institute - Antoni van Leeuwenhoek Hospital, Amsterdam, 1066 CX, The Netherlands.

⁷⁴ Department of Laboratory Medicine and Pathology, Mayo Clinic, Rochester, MN, 55905, USA.

⁷⁵ Academic Unit of Pathology, Department of Neuroscience, University of Sheffield, Sheffield, S10 2TN, UK.

⁷⁶ Department of Medical Epidemiology and Biostatistics, Karolinska Institutet, Stockholm, 171 65, Sweden.

⁷⁷ Department of Clinical Genetics, Fox Chase Cancer Center, Philadelphia, PA, 19111, USA.

⁷⁸ Department of Pathology, Leiden University Medical Center, Leiden, 2333 ZA, The Netherlands.

⁷⁹ Department of Human Genetics, Leiden University Medical Center, Leiden, 2333 ZA, The Netherlands.

⁸⁰ Department of Medical Oncology, Vall d'Hebron Institute of Oncology (VHIO), University Hospital, Vall d'Hebron, Barcelona, 08035, Spain.

⁸¹ Department of Population Sciences, Beckman Research Institute of City of Hope, Duarte, CA, 91010, USA.

⁸² Centre for Epidemiology and Biostatistics, Melbourne School of Population and Global Health, The University of Melbourne, Melbourne, Victoria, 3010, Australia.

⁸³ Department of Medicine, Abramson Cancer Center, Perelman School of Medicine at the University of Pennsylvania, Philadelphia, PA, 19104, USA.

⁸⁴ Department of Non-Communicable Disease Epidemiology, London School of Hygiene and Tropical Medicine, London, WC1E 7HT, UK.

⁸⁵ Département de Médecine Moléculaire, Faculté de Médecine, Centre Hospitalier Universitaire de Québec Research Center, Laval University, Québec City, QC, G1V 0A6, Canada.

⁸⁶ Precision Medicine, School of Clinical Sciences at Monash Health, Monash University, Clayton, Victoria, 3168, Australia.

⁸⁷ Cáncer Hereditario, Instituto de Biología y Genética Molecular, IBGM, Universidad de Valladolid, Centro Superior de Investigaciones Científicas, UVA-CSIC, Valladolid, 47003, Spain.

⁸⁸ Southampton Clinical Trials Unit, Faculty of Medicine, University of Southampton, Southampton, SO17 1BJ, UK.

⁸⁹ Cancer Sciences Academic Unit, Faculty of Medicine, University of Southampton, Southampton, SO17 1BJ, UK.

⁹⁰ Department of Biomedical Sciences, Faculty of Science and Technology, University of Westminster, London, W1B 2HW, UK.

⁹¹ Institute for Medical Informatics, Statistics and Epidemiology, University of Leipzig, Leipzig, 04107, Germany.

⁹² LIFE - Leipzig Research Centre for Civilization Diseases, University of Leipzig, Leipzig, 04103, Germany.

⁹³ Division of Evolution and Genomic Medicine, School of Biological Sciences, Faculty of Biology, Medicine and Health, University of Manchester, Manchester Academic Health Science Centre, Manchester, M13 9WL, UK.

⁹⁴ Manchester Centre for Genomic Medicine, St Mary's Hospital, Manchester University Hospitals NHS Foundation Trust, Manchester Academic Health Science Centre, Manchester, M13 9WL, UK.

⁹⁵ David Geffen School of Medicine, Department of Medicine Division of Hematology and Oncology, University of California at Los Angeles, Los Angeles, CA, 90095, USA.

⁹⁶ Department of Gynecology and Obstetrics, Comprehensive Cancer Center ER-EMN, University Hospital Erlangen, Friedrich-Alexander-University Erlangen-Nuremberg, Erlangen, 91054, Germany.

⁹⁷ The Breast Cancer Now Toby Robins Research Centre, The Institute of Cancer Research, London, SW7 3RP, UK.

⁹⁸ Leuven Multidisciplinary Breast Center, Department of Oncology, Leuven Cancer Institute, University Hospitals Leuven, Leuven, 3000, Belgium.

⁹⁹ Department of Breast Surgery, Herlev and Gentofte Hospital, Copenhagen University Hospital, Herlev, 2730, Denmark.

¹⁰⁰ Department of Cancer Epidemiology and Genetics, Masaryk Memorial Cancer Institute, Brno, 65653, Czech Republic.

¹⁰¹ Program in Cancer Genetics, Departments of Human Genetics and Oncology, McGill University, Montr al, QC, H4A 3J1, Canada.

¹⁰² The Susanne Levy Gertner Oncogenetics Unit, Chaim Sheba Medical Center, Ramat Gan, 52621, Israel.

¹⁰³ Sackler Faculty of Medicine, Tel Aviv University, Ramat Aviv, 69978, Israel.

- ¹⁰⁴ School of Public Health, Curtin University, Perth, Western Australia, 6102, Australia.
- ¹⁰⁵ Genomic Medicine Group, Galician Foundation of Genomic Medicine, Instituto de Investigación Sanitaria de Santiago de Compostela (IDIS), Complejo Hospitalario Universitario de Santiago, SERGAS, Santiago de Compostela, 15706, Spain.
- ¹⁰⁶ Moores Cancer Center, University of California San Diego, La Jolla, CA, 92037, USA.
- ¹⁰⁷ Section of Molecular Genetics, Department of Laboratory Medicine, University Hospital of Pisa, Pisa, Italy.
- ¹⁰⁸ Schools of Medicine and Public Health, Division of Cancer Prevention & Control Research, Jonsson Comprehensive Cancer Centre, UCLA, Los Angeles, CA, 90096-6900, USA.
- ¹⁰⁹ Cancer Risk and Prevention Clinic, Dana-Farber Cancer Institute, Boston, MA, 02215, USA.
- ¹¹⁰ Department of Medical Oncology, University Hospital of Heraklion, Heraklion, 711 10, Greece.
- ¹¹¹ Cancer Epidemiology & Intelligence Division, Cancer Council Victoria, Melbourne, Victoria, 3004, Australia.
- ¹¹² Department of Epidemiology and Preventive Medicine, Monash University, Melbourne, Victoria, 3004, Australia.
- ¹¹³ Department of Pathology and Laboratory Medicine, Kansas University Medical Center, Kansas City, KS, 66160, USA.
- ¹¹⁴ Department of Medicine, McGill University, Montréal, QC, H4A 3J1, Canada.
- ¹¹⁵ Division of Clinical Epidemiology, Royal Victoria Hospital, McGill University, Montréal, QC, H4A 3J1, Canada.
- ¹¹⁶ Department of Dermatology, Huntsman Cancer Institute, University of Utah School of Medicine, Salt Lake City, UT, 84112, USA.

- ¹¹⁷ Clinical Genetics Branch, Division of Cancer Epidemiology and Genetics, National Cancer Institute, Bethesda, MD, 20850-9772, USA.
- ¹¹⁸ Department of Surgery, Oulu University Hospital, University of Oulu, Oulu, 90220, Finland.
- ¹¹⁹ Centre de Recherche du Centre Hospitalier de Université de Montréal (CHUM), Université de Montréal, Montréal, QC, H2X 0A9, Canada.
- ¹²⁰ Cancer & Environment Group, Center for Research in Epidemiology and Population Health (CESP), INSERM, University Paris-Sud, University Paris-Saclay, Villejuif, 94805, France.
- ¹²¹ Center for Hereditary Breast and Ovarian Cancer, University Hospital of Cologne, Cologne, 50937, Germany.
- ¹²² Center for Molecular Medicine Cologne (CMMC), University of Cologne, Cologne, 50931, Germany.
- ¹²³ Department of Preventive Medicine, Keck School of Medicine, University of Southern California, Los Angeles, CA, 90033, USA.
- ¹²⁴ Institute of Environmental Medicine, Karolinska Institutet, Stockholm, 171 77, Sweden.
- ¹²⁵ Department of Oncology, Södersjukhuset, Stockholm, 118 83, Sweden.
- ¹²⁶ Molecular Genetics of Breast Cancer, German Cancer Research Center (DKFZ), Heidelberg, 69120, Germany.
- ¹²⁷ Translational Cancer Research Area, University of Eastern Finland, Kuopio, 70210, Finland.
- ¹²⁸ Institute of Clinical Medicine, Pathology and Forensic Medicine, University of Eastern Finland, Kuopio, 70210, Finland.
- ¹²⁹ Imaging Center, Department of Clinical Pathology, Kuopio University Hospital, Kuopio, 70210, Finland.

- ¹³⁰ Saw Swee Hock School of Public Health, National University of Singapore, Singapore, 119077, Singapore.
- ¹³¹ Department of Surgery, National University Health System, Singapore, 119228, Singapore.
- ¹³² Department of Medical Oncology, Family Cancer Clinic, Erasmus MC Cancer Institute, Rotterdam, 3015 CN, The Netherlands.
- ¹³³ School of Population and Global Health, The University of Western Australia, Perth, Western Australia, 6009, Australia.
- ¹³⁴ Family Cancer Clinic, The Netherlands Cancer Institute - Antoni van Leeuwenhoek hospital, Amsterdam, 1066 CX, The Netherlands.
- ¹³⁵ Division of Cancer Sciences, University of Manchester, Manchester, M13 9PL, UK.
- ¹³⁶ Center for Medical Genetics, NorthShore University HealthSystem, Evanston, IL, 60201, USA.
- ¹³⁷ The University of Chicago Pritzker School of Medicine, Chicago, IL, 60637, USA.
- ¹³⁸ N.N. Petrov Institute of Oncology, St. Petersburg, 197758, Russia.
- ¹³⁹ Australian Breast Cancer Tissue Bank, Westmead Institute for Medical Research, University of Sydney, Sydney, New South Wales, 2145, Australia.
- ¹⁴⁰ The Hereditary Breast and Ovarian Cancer Research Group Netherlands (HEBON), Coordinating center: The Netherlands Cancer Institute, Amsterdam, 1066 CX, The Netherlands.
- ¹⁴¹ Lombardi Comprehensive Cancer Center, Georgetown University, Washington, DC, 20007, USA.
- ¹⁴² Division of Epidemiology, Center for Public Health Sciences, National Cancer Center, Tokyo, 104-0045, Japan.
- ¹⁴³ Research Centre for Genetic Engineering and Biotechnology 'Georgi D. Efremov', Macedonian Academy of Sciences and Arts, Skopje, 1000, Republic of Macedonia.

- ¹⁴⁴ Independent Laboratory of Molecular Biology and Genetic Diagnostics, Pomeranian Medical University, Szczecin, 71-252, Poland.
- ¹⁴⁵ Parkville Familial Cancer Centre, Peter MacCallum Cancer Center, Melbourne, Victoria, 3000, Australia.
- ¹⁴⁶ Hematology, oncology and transfusion medicine center, Dept. of Molecular and Regenerative Medicine, Vilnius University Hospital Santariskiu Clinics, Vilnius, Lithuania.
- ¹⁴⁷ Department of Medicine, Division of Hematology/Oncology, UPMC Hillman Cancer Center; University of Pittsburgh School of Medicine, Pittsburgh, PA 15232, USA.
- ¹⁴⁸ Department of Medicine, Division of Oncology, Stanford Cancer Institute, Stanford University School of Medicine, Stanford, CA, 94304, USA.
- ¹⁴⁹ Division of Genetics and Epidemiology, The Institute of Cancer Research, London, SM2 5NG, UK.
- ¹⁵⁰ Department of Oncology, Tampere University Hospital, Tampere, 33521, Finland.
- ¹⁵¹ Division of Cancer Epidemiology, German Cancer Research Center (DKFZ), Heidelberg, 69120, Germany.
- ¹⁵² Department of Preventive Medicine, Seoul National University College of Medicine, Seoul, 03080, Korea.
- ¹⁵³ Department of Biomedical Sciences, Seoul National University Graduate School, Seoul, 03080, Korea.
- ¹⁵⁴ Cancer Research Institute, Seoul National University, Seoul, 03080, Korea.
- ¹⁵⁵ Women's Cancer Program at the Samuel Oschin Comprehensive Cancer Institute, Cedars-Sinai Medical Center, Los Angeles, CA, 90048, USA.
- ¹⁵⁶ Surgery, School of Medicine, National University of Ireland, Galway, H91TK33, Ireland.
- ¹⁵⁷ Department of Genetics and Fundamental Medicine, Bashkir State University, Ufa, 450076, Russia.

- ¹⁵⁸ Department of Obstetrics and Gynecology, Helsinki University Hospital, University of Helsinki, Helsinki, 00290, Finland.
- ¹⁵⁹ Familial Cancer Service, Weatmead Hospital, Wentworthville, New South Wales, 2145, Australia.
- ¹⁶⁰ Radiation Epidemiology Branch, Division of Cancer Epidemiology and Genetics, National Cancer Institute, Bethesda, MD, 20892, USA.
- ¹⁶¹ Department of Internal Medicine, Evangelische Kliniken Bonn gGmbH, Johanniter Krankenhaus, Bonn, 53177, Germany.
- ¹⁶² Molecular Diagnostics Laboratory, INRASTES, National Centre for Scientific Research 'Demokritos', Athens, 15310, Greece.
- ¹⁶³ Division of Cancer Epidemiology and Genetics, National Cancer Institute, National Institutes of Health, Department of Health and Human Services, Bethesda, MD, 20850, USA.
- ¹⁶⁴ Department of Histopathology and Cytology, Clinical Hospital Acibadem Sistina, Skopje, 1000, Republic of Macedonia.
- ¹⁶⁵ Hong Kong Hereditary Breast Cancer Family Registry, Cancer Genetics Centre, Happy Valley, Hong Kong.
- ¹⁶⁶ Department of Surgery, The University of Hong Kong, Pok Fu Lam, Hong Kong.
- ¹⁶⁷ Department of Surgery, Hong Kong Sanatorium and Hospital, Happy Valley, Hong Kong.
- ¹⁶⁸ VIB Center for Cancer Biology, VIB, Leuven, 3001, Belgium.
- ¹⁶⁹ Laboratory for Translational Genetics, Department of Human Genetics, University of Leuven, Leuven, 3000, Belgium.
- ¹⁷⁰ Genetic Epidemiology of Cancer team, Inserm U900, Paris, 75005, France.
- ¹⁷¹ Department of Molecular Medicine and Surgery, Karolinska Institutet, Stockholm, 171 76, Sweden.

- ¹⁷² Department of Clinical Genetics, Karolinska University Hospital, Stockholm, 171 76, Sweden.
- ¹⁷³ Division of Health Sciences, Warwick Medical School, University of Warwick, Coventry, CV4 7AL, UK.
- ¹⁷⁴ Institute of Population Health, University of Manchester, Manchester, M13 9PL, UK.
- ¹⁷⁵ Department of Clinical Science and Education, Södersjukhuset, Karolinska Institutet, Stockholm, 118 83, Sweden.
- ¹⁷⁶ Department of Family Medicine and Public Health, University of California San Diego, La Jolla, CA, 92093, USA.
- ¹⁷⁷ Division of Molecular Medicine, Aichi Cancer Center Research Institute, Nagoya, 464-8681, Japan.
- ¹⁷⁸ Department of Epidemiology, Nagoya University Graduate School of Medicine, Nagoya, 466-8550, Japan.
- ¹⁷⁹ Cancer Epidemiology Group, University Cancer Center Hamburg (UCCH), University Medical Center Hamburg-Eppendorf, Hamburg, 20246, Germany.
- ¹⁸⁰ Anatomical Pathology, The Alfred Hospital, Melbourne, Victoria, 3004, Australia.
- ¹⁸¹ Department of Gynecology and Obstetrics, Ludwig Maximilian University of Munich, Munich, 80336, Germany.
- ¹⁸² Faculty of Medicine, University of Heidelberg, Heidelberg, 69120, Germany.
- ¹⁸³ NRG Oncology, Statistics and Data Management Center, Roswell Park Cancer Institute, Buffalo, NY, 14263, USA.
- ¹⁸⁴ Department of Laboratory Medicine and Pathobiology, University of Toronto, Toronto, ON, M5S 1A8, Canada.
- ¹⁸⁵ Laboratory Medicine Program, University Health Network, Toronto, ON, M5G 2C4, Canada.
- ¹⁸⁶ Radiation Oncology, Hospital Meixoeiro-XXI de Vigo, Vigo, 36214, Spain.

¹⁸⁷ Women's College Research Institute, University of Toronto, Toronto, ON, M5S 1A8, Canada.

¹⁸⁸ Department of Biochemistry and Molecular Medicine, University of California Davis, Davis, CA, 95817, USA.

¹⁸⁹ Center for Genomic Medicine, Rigshospitalet, Copenhagen University Hospital, Copenhagen, DK-2100, Denmark.

¹⁹⁰ Latvian Biomedical Research and Study Centre, Riga, Latvia.

¹⁹¹ Department of Health Sciences Research, Mayo Clinic, Rochester, MN, 55905, USA.

¹⁹² Clinical Genetics Research Lab, Department of Cancer Biology and Genetics, Memorial Sloan-Kettering Cancer Center, New York, NY, 10065, USA.

¹⁹³ Clinical Genetics Service, Department of Medicine, Memorial Sloan-Kettering Cancer Center, New York, NY, 10065, USA.

¹⁹⁴ Department of Molecular Genetics, National Institute of Oncology, Budapest, 1122, Hungary.

¹⁹⁵ Center for Clinical Cancer Genetics, The University of Chicago, Chicago, IL, 60637, USA.

¹⁹⁶ Department of Cancer Epidemiology, Clinical Sciences, Lund University, Lund, 222 42, Sweden.

¹⁹⁷ Centre for Cancer Research and Cell Biology, Queen's University Belfast, Belfast, Ireland, BT7 1NN, UK.

¹⁹⁸ University of New Mexico Health Sciences Center, University of New Mexico, Albuquerque, NM, 87131, USA.

¹⁹⁹ Cancer Research UK Clinical Trials Unit, Institute of Cancer Sciences, University of Glasgow, Glasgow, G12 0YN, UK.

²⁰⁰ Section of Molecular Diagnostics, Clinical Biochemistry, Aalborg University Hospital, Aalborg, 9000, Denmark.

- ²⁰¹ Genome Diagnostics Program, IFOM - the FIRC (Italian Foundation for Cancer Research) Institute of Molecular Oncology, Milan, 20139, Italy.
- ²⁰² Translational Research Laboratory, IDIBELL (Bellvitge Biomedical Research Institute), Catalan Institute of Oncology, CIBERONC, Barcelona, 08908, Spain.
- ²⁰³ Laboratory of Cancer Genetics and Tumor Biology, Cancer and Translational Medicine Research Unit, Biocenter Oulu, University of Oulu, Oulu, 90570, Finland.
- ²⁰⁴ Laboratory of Cancer Genetics and Tumor Biology, Northern Finland Laboratory Centre Oulu, Oulu, 90570, Finland.
- ²⁰⁵ Unit of Molecular Bases of Genetic Risk and Genetic Testing, Department of Research, Fondazione IRCCS (Istituto Di Ricovero e Cura a Carattere Scientifico) Istituto Nazionale dei Tumori (INT), Milan, 20133, Italy.
- ²⁰⁶ School of Women's and Children's Health, Faculty of Medicine, University of NSW Sydney, Sydney, New South Wales, 2052, Australia.
- ²⁰⁷ The Kinghorn Cancer Centre, Garvan Institute of Medical Research, Sydney, New South Wales, 2010, Australia.
- ²⁰⁸ Clinical Genetics, Karolinska Institutet, Stockholm, 171 76, Sweden.
- ²⁰⁹ Clalit National Cancer Control Center, Carmel Medical Center and Technion Faculty of Medicine, Haifa, 35254, Israel.
- ²¹⁰ Chronic Disease Epidemiology, Yale School of Public Health, New Haven, CT, 06510, USA.
- ²¹¹ Medical Oncology Department, Hospital Universitario Puerta de Hierro, Madrid, 28222, Spain.
- ²¹² Department of Oncology, University Hospital of Larisa, Larisa, 411 10, Greece.

- ²¹³ Epidemiology Branch, National Institute of Environmental Health Sciences, NIH, Research Triangle Park, NC, 27709, USA.
- ²¹⁴ Fundación Pública Galega Medicina Xenómica, Santiago De Compostela, 15706, Spain.
- ²¹⁵ Instituto de Investigación Sanitaria de Santiago de Compostela, Santiago De Compostela, 15706, Spain.
- ²¹⁶ School of Medicine, University of Western Australia, Perth, Western Australia, Australia.
- ²¹⁷ Research Oncology, Guy's Hospital, King's College London, London, SE1 9RT, UK.
- ²¹⁸ Faculty of Information Technology, Monash University, Melbourne, Victoria, 3800, Australia.
- ²¹⁹ National Center for Tumor Diseases, University Hospital and German Cancer Research Center, Heidelberg, 69120, Germany.
- ²²⁰ Network Aging Research, University of Heidelberg, Heidelberg, 6915, Germany.
- ²²¹ Division of Molecular Medicine, Pathology North, John Hunter Hospital, Newcastle, New South Wales, 2305, Australia.
- ²²² Discipline of Medical Genetics, School of Biomedical Sciences and Pharmacy, Faculty of Health, University of Newcastle, Callaghan, New South Wales, 2308, Australia.
- ²²³ Hunter Medical Research Institute, John Hunter Hospital, Newcastle, New South Wales, 2305, Australia.
- ²²⁴ Clinical Cancer Genetics Program, Division of Human Genetics, Department of Internal Medicine, The Comprehensive Cancer Center, The Ohio State University, Columbus, OH, 43210, USA.
- ²²⁵ Department of Internal Medicine, Division of Oncology, University of Kansas Medical Center, Westwood, KS, 66205, USA.
- ²²⁶ Institute of Biomedical Sciences, Academia Sinica, Taipei, 115, Taiwan.

- ²²⁷ School of Public Health, China Medical University, Taichung, Taiwan.
- ²²⁸ Dept of OB/GYN and Comprehensive Cancer Center, Medical University of Vienna, Vienna, 1090, Austria.
- ²²⁹ Clinical Cancer Genetics, City of Hope, Duarte, CA, 91010, USA.
- ²³⁰ Ss. Cyril and Methodius University in Skopje, Medical Faculty, University Clinic of Radiotherapy and Oncology, Skopje, 1000, Republic of Macedonia.
- ²³¹ Department of Clinical Pathology, The University of Melbourne, Melbourne, Victoria, 3010, Australia.
- ²³² Population Oncology, BC Cancer, Vancouver, BC, V5Z 1G1, Canada.
- ²³³ School of Population and Public Health, University of British Columbia, Vancouver, BC, V6T 1Z4, Canada.
- ²³⁴ The Curtin UWA Centre for Genetic Origins of Health and Disease, Curtin University and University of Western Australia, Perth, Western Australia, 6000, Australia.
- ²³⁵ Service de Génétique, Institut Curie, Paris, 75005, France.
- ²³⁶ Université Paris Descartes, Paris, 75006, France.
- ²³⁷ Institute of Human Genetics, University Hospital Heidelberg, Heidelberg, 69120, Germany.
- ²³⁸ Division of Breast Cancer Research, The Institute of Cancer Research, London, SW7 3RP, UK.
- ²³⁹ Channing Division of Network Medicine, Department of Medicine, Brigham and Women's Hospital, Harvard Medical School, Boston, MA, 02115, USA.
- ²⁴⁰ Dept of OB/GYN, Medical University of Vienna, Vienna, 1090, Austria.
- ²⁴¹ Faculty of Medicine, University of Southampton, Southampton, SO17 1BJ, UK.

²⁴² Epigenetic and Stem Cell Biology Laboratory, National Institute of Environmental Health Sciences, NIH, Research Triangle Park, NC, 27709, USA.

²⁴³ Department of Genetics, Portuguese Oncology Institute, Porto, 4220-072, Portugal.

²⁴⁴ Biomedical Sciences Institute (ICBAS), University of Porto, Porto, 4050-013, Portugal.

²⁴⁵ Cancer Center, Kuopio University Hospital, Kuopio, 70210, Finland.

²⁴⁶ Institute of Clinical Medicine, Oncology, University of Eastern Finland, Kuopio, 70210, Finland.

²⁴⁷ Cancer Research Malaysia, Subang Jaya, Selangor, 47500, Malaysia.

²⁴⁸ Breast Cancer Research Unit, Cancer Research Institute, University Malaya Medical Centre, Kuala Lumpur, 59100, Malaysia.

²⁴⁹ Department of Epidemiology, Mailman School of Public Health, Columbia University, New York, NY, 10032, USA.

²⁵⁰ Genetic Counseling Unit, Hereditary Cancer Program, IDIBELL (Bellvitge Biomedical Research Institute), Catalan Institute of Oncology, CIBERONC, Barcelona, 08908, Spain.

²⁵¹ Department of Clinical Genetics, Odense University Hospital, Odense C, 5000, Denmark.

²⁵² Department of Medicine, Magee-Womens Hospital, University of Pittsburgh School of Medicine, Pittsburgh, PA, 15213, USA.

²⁵³ UO Anatomia Patologica, Ospedale di Circolo-Universit  dell'Insubria, Varese, 21100, Italy.

²⁵⁴ Department of Medical Genetics, University of Cambridge, Cambridge, CB2 0QQ, UK.

²⁵⁵ Department of Cancer Biology and Genetics, The Ohio State University, Columbus, OH, 43210, USA.

²⁵⁶ Department of Surgery, Leiden University Medical Center, Leiden, 2333 ZA, The Netherlands.

²⁵⁷ Institute of Cancer and Genomic Sciences, University of Birmingham, Birmingham, B15 2TT, UK.

- ²⁵⁸ Wellcome Trust Centre for Human Genetics and Oxford NIHR Biomedical Research Centre, University of Oxford, Oxford, OX3 7BN, UK.
- ²⁵⁹ Center for Population Health Research, National Institute of Public Health, Mexico, 62100, Mexico.
- ²⁶⁰ Department of Epidemiology, Gillings School of Global Public Health and UNC Lineberger Comprehensive Cancer Center, University of North Carolina at Chapel Hill, Chapel Hill, NC, USA.
- ²⁶¹ Department of Medical Oncology, Beth Israel Deaconess Medical Center, Boston, MA, 02215, USA.
- ²⁶² Department of Pathology, University Hospital of Heraklion, Heraklion, 711 10, Greece.
- ²⁶³ Frauenklinik der Stadtklinik Baden-Baden, Baden-Baden, 76532, Germany.
- ²⁶⁴ Department of Health Science Research, Division of Epidemiology, Mayo Clinic, Rochester, MN, 55905, USA.
- ²⁶⁵ Department of Clinical Genetics, Leiden University Medical Center, Leiden, 2333 ZA, The Netherlands.
- ²⁶⁶ Department of Genetics, University of Pretoria, Arcadia, 0007, South Africa.
- ²⁶⁷ Division of Functional onco-genomics and genetics, Centro di Riferimento Oncologico di Aviano (CRO), IRCCS, Aviano, 33081, Italy.
- ²⁶⁸ Department of Pathology, Netherlands Cancer Institute, 1006 BE,
- ²⁶⁹ Biostatistics and Computational Biology Branch, National Institute of Environmental Health Sciences, NIH, Research Triangle Park, NC, 27709, USA.
- ²⁷⁰ Department of Surgical Sciences, Uppsala University, Uppsala, 751 05, Sweden.
- ²⁷¹ Division of Genetics and Epidemiology, Institute of Cancer Research, London, SM2 5NG, UK.
- ²⁷² Division of Psychosocial Research and Epidemiology, The Netherlands Cancer Institute - Antoni van Leeuwenhoek hospital, Amsterdam, 1066 CX, The Netherlands.

²⁷³ Department of Cancer Genetics, Institute for Cancer Research, Oslo University Hospital-Radiumhospitalet, Oslo, 0379, Norway.

²⁷⁴ Institute of Clinical Medicine, Faculty of Medicine, University of Oslo, Oslo, 0450, Norway.

²⁷⁵ These authors contributed equally.

²⁷⁶ Senior author.

* Correspondence: pkraft@hsph.harvard.edu (PK), amd24@medschl.cam.ac.uk (AMD)

ABSTRACT

Genome-wide association studies have identified breast cancer risk variants in over 150 genomic regions, but the mechanisms underlying risk remain largely unknown. These regions were explored by combining association analysis with *in silico* genomic feature annotations. We defined 205 independent risk-associated signals with the set of credible causal variants (CCVs) in each one. In parallel, we used a Bayesian approach (PAINTOR) that combines genetic association, linkage disequilibrium, and enriched genomic features to determine variants with high posterior probabilities (HPPs) of being causal. Potentially causal variants were significantly over-represented in active gene regulatory regions and transcription factor binding sites. We applied our INQUSIT pipeline for prioritizing genes as targets of potentially causal variants, using gene expression (eQTL), chromatin interaction and functional annotations. Known cancer drivers, transcription factors and genes in the developmental, apoptosis, immune system and DNA integrity checkpoint gene ontology pathways, were over-represented among the 178 highest confidence target genes.

INTRODUCTION

Genome-wide association studies (GWAS) have identified genetic variants associated with breast cancer risk in more than 150 genomic regions^{1,2}. However, the variants and genes driving these associations are mostly unknown, with fewer than 20 regions studied in detail³⁻²⁰. Here, we aimed to fine-map all known breast cancer susceptibility regions using dense genotype data on > 217K subjects participating in the Breast Cancer Association Consortium (BCAC) and the Consortium of Investigators of Modifiers of *BRCA1/2* (CIMBA). All samples were genotyped using the OncoArrayTM^{1,2,21} or the iCOGS chip^{22,23}. Stepwise multinomial logistic regression was used to identify independent association signals in each region and define credible causal variants (CCVs) within each signal. We found genomic features significantly overlapping the CCVs and then used a Bayesian approach, integrating informative genomic features and genetic associations, to refine the set of likely causal variants and calculate their posterior probabilities. Finally, we integrated genetic and *in silico* epigenetic, expression and chromatin conformation data to infer the likely target genes of each signal.

RESULTS

Most breast cancer genomic regions contain multiple independent risk-associated signals

We included 109,900 breast cancer cases and 88,937 controls, all of European ancestry, from 75 studies in the BCAC. Genotypes (directly observed or imputed) were available for 639,118 single nucleotide polymorphisms (SNPs), deletion/insertions, and copy number variants (CNVs) with minor allele frequency (MAF) $\geq 0.1\%$ within 152, previously defined, risk-associated regions (**Supplementary Table 1; Figure 1**). Multivariate logistic regression confirmed associations for 150/152 regions at a p-value $< 10^{-4}$ significance threshold (**Supplementary Table 2A**). To determine the number of independent risk

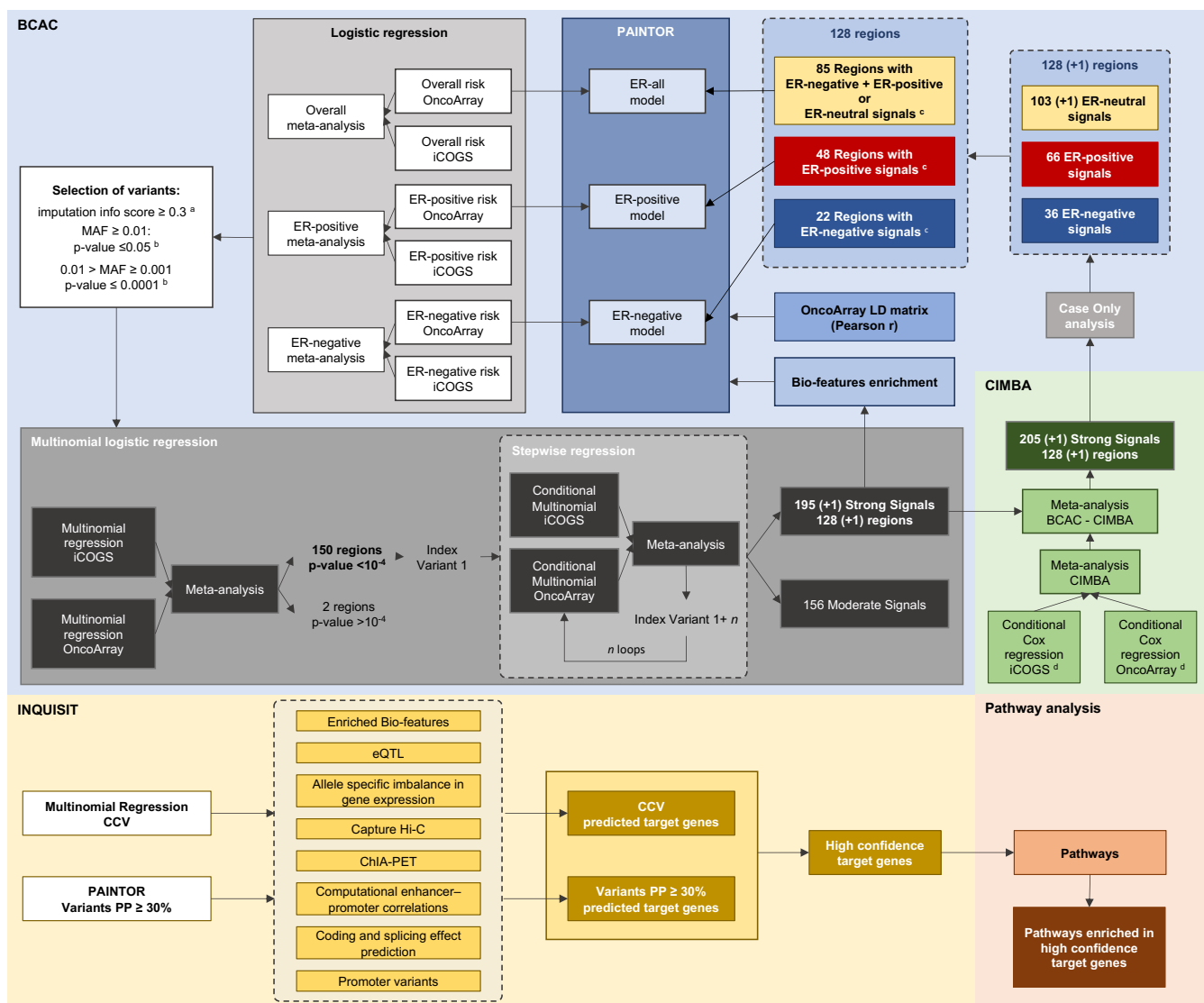


Figure 1. Flowchart summarizing the study design. ^a In iCOGS and in OncoArray; ^b for at least one phenotype; ^c regions containing signals associated with more than one phenotype were evaluated with more than one PAINTOR model; ^d conditional on the index variants from BCAC strong signals.

signals within each region we applied stepwise multinomial logistic regression, deriving the association of each variant, conditional on the more significant ones, in order of statistical significance. Finally, we defined CCVs in each signal as variants with conditional p-values within two orders of magnitude of the

index variant ²⁴. We classified the evidence for each independent signal, and its CCVs, as either *strong* (conditional p-values $<10^{-6}$) or *moderate* ($10^{-6} < \text{conditional p-values} < 10^{-4}$).

From the 150 genomic regions we identified 352 independent risk signals containing 13,367 CCVs, 7,394 of these were within the 196 strong-evidence signals across 129 regions (**Figures 2A-B**). The number of signals per region ranged from 1 to 9, with 79 (53%) containing multiple signals. We noted a wide range of CCVs per signal, but in 42 signals there was only a single CCV and this was assumed to be causal (**Figures 2C-D, Table 1**).

The majority of breast tumors express the estrogen receptor (ER-positive), but ~20% do not (ER-negative); these two tumor types have distinct biological and clinical characteristics ²⁵. Using a case-only analysis for the 196 strong-evidence signals, we found 66 signals (34%; containing 1,238 CCVs) where the lead variant conferred a greater relative-risk of developing ER-positive tumors (false discovery rate, FDR 5%), and 29 (15%; 646 CCVs) where the lead variant conferred a greater risk of ER-negative cancer tumors (FDR 5%) (**Supplementary Table 2B, Figure 2E**). The remaining 101 signals (51%, 5,510 CCVs) showed no difference by ER status (referred to as ER-neutral).

Patients with *BRCA1* mutations are more likely to develop ER-negative tumors ²⁶. Hence, to increase our power to identify ER-negative signals, we performed a fixed-effects meta-analysis, combining association results from *BRCA1* mutation carriers in CIMBA with the BCAC ER-negative association results. This meta-analysis identified ten additional signals, seven ER-negative and three ER-neutral,

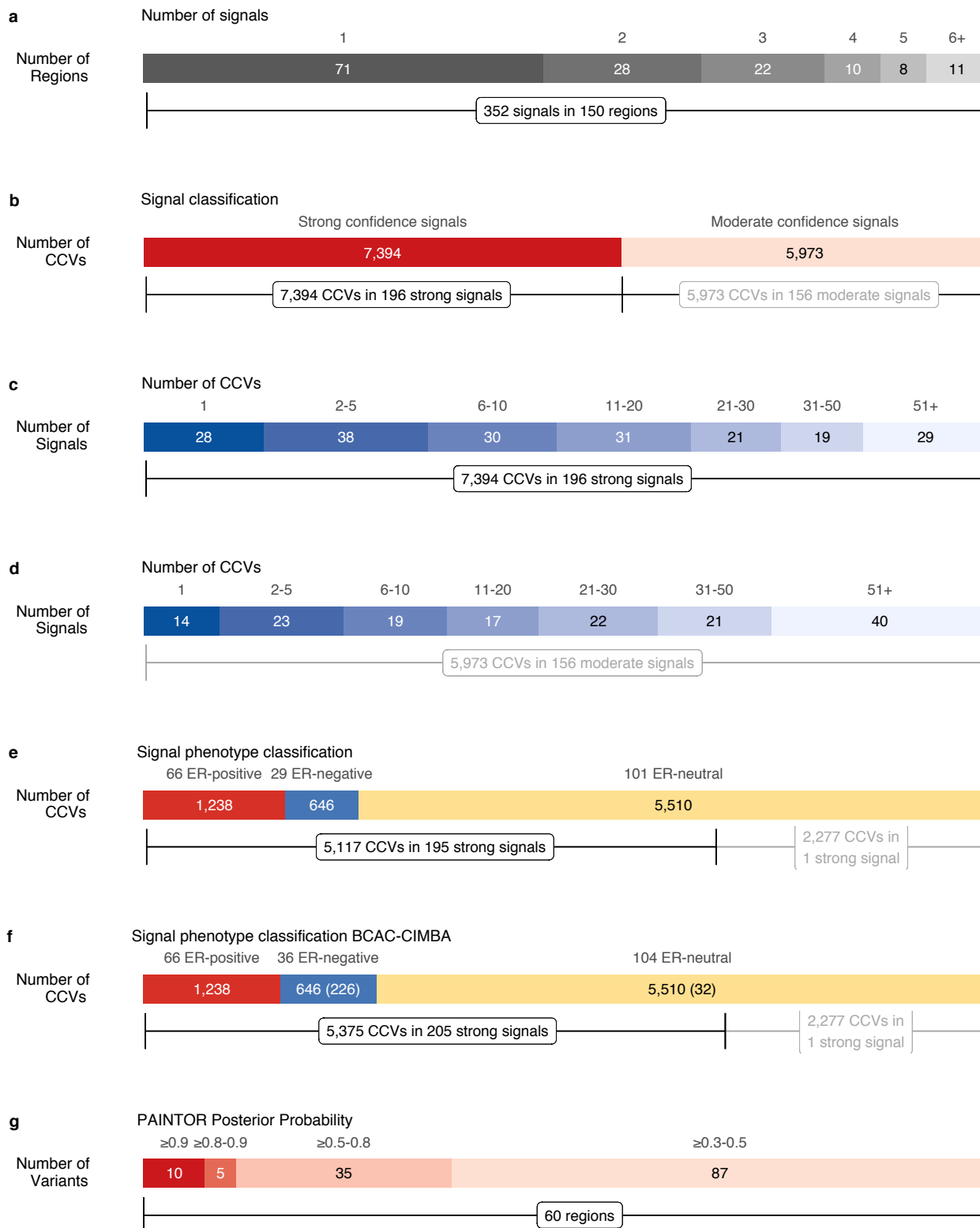


Figure 2. Determining independent risk signals and credible candidate variants (CCVs). (a) Number of independent signals per region identified through multinomial stepwise logistic regression. (b) Signal classification according to their confidence into strong and moderate confidence signals. (c) Number of CCVs per signal at strong confidence signals identified through multinomial stepwise logistic regression. (d) Number of CCVs per signal at moderate confidence signals identified through multinomial stepwise regression. (e) Subtype classification of strong signals into ER-positive, ER-negative and signals equally associated with both phenotypes (ER-neutral) from BCAC analysis. (f) Subtype classification from the meta-analysis of BCAC and CIMBA. Between brackets, number of CCVs from the meta-analysis of BCAC and CIMBA. (g) Number of variants at different posterior probability thresholds. 15 variants reach a PP $\geq 80\%$ by at least one of the three models (ER-all, ER-positive, ER-negative).

making 206 strong-evidence signals (17% ER-negative) containing 7,652 CCVs in total (**Figure 2F**). More than one quarter of the CCVs (2,277) were accounted for by one signal, resulting from strong linkage disequilibrium with a copy number variant. The remaining analyses focused on the other 205 strong signals across 128 regions (**Supplementary Table 2C**).

CCVs are over-represented in active gene-regulatory regions and transcription factor binding sites (TFBSs)

We constructed a database of mapped genomic-features in seven primary cells derived from normal breast and 19 breast cell lines using publicly available data, resulting in 811 annotation tracks in total. These ranged from general features, such as whether a variant was in an exon or in open chromatin, to more specific features, such a cell-specific TF binding or histone mark (determined through ChIP-Seq experiments) in breast-derived cells or cell lines. Using logistic regression, we examined the overlap of these genomic-features with the positions of 5,117 CCVs in the 195 strong-evidence BCAC signals versus the positions of 622,903 variants excluded as credible candidates in the same regions (**Supplementary**

Figure 1A, Supplementary Table 3). We found significant enrichment of CCVs (FDR 5%) in the following genomic-features:

(i) Open chromatin (determined by DNase-seq and FAIRE-seq) in ER-positive breast cancer cell-lines and normal breast (**Figure 3A**). Conversely, we found depletion of CCVs within heterochromatin (determined by the H3K9me3 mark in normal breast, and by chromatin-state in ER-positive cells ²⁷).

(ii) Actively transcribed genes in normal breast and ER-positive cell lines (defined by H3K36me3 or H3K79me2 histone marks, **Figure 3A**). Enrichment was larger for ER-neutral CCVs than for those affecting either ER-positive or ER-negative tumors.

(iii) Gene regulatory regions. CCVs overlapped distal gene regulatory elements in ER-positive breast cancer cells lines (defined by H3K4me1 or H3K27ac marks, **Figure 3B**). This was confirmed using the ENCODE definition of active enhancers in MCF-7 cells (enhancer-like regions defined by combining DNase and H3K27ac marks), as well as the definition of ²⁸ and ²⁷ (Supplementary Table 3). Under these more stringent definitions, enrichment among ER-positive CCVs was significantly larger than ER-negative or ER-neutral CCVs. Data from ²⁷, showed that 73% of active enhancer regions overlapped by ER-positive CCVs in ER-positive cells (MCF-7), are inactive in the normal HMEC breast cell line; thus, these enhancers appear to be MCF-7-specific.

We also detected significant enrichment of CCVs in active promoters in ER-positive cells (defined by H3K4me3 marks in T-47D), although the evidence for this effect was weaker than for distal regulatory elements (defined by H3K27ac marks in MCF-7, **Figure 3B**). Only ER-positive CCVs were significantly

Figure 3. Overlap of CCVs with gene regulatory regions gene bodies and transcription factor binding sites. (a) Breast cancer CCVs overlap with chromatin states and broad breast cells epigenetic marks. (b) Breast cancer CCVs overlap with breast cells epigenetic marks. (c) Autoimmune CCVs overlap with breast cells epigenetic marks. (d) Breast cancer CCVs overlap with autoimmune-related epigenetic marks. (e) Autoimmune CCVs overlap with autoimmune-related epigenetic marks. (f) Significant ER-positive CCVs overlap with transcription factors binding sites. TFBSs found significant for ER-positive CCVs are highlighted in red (x axis labels). (g) Significant ER-negative CCVs overlap with transcription factors binding sites. (h) Significant ER-neutral CCVs overlap with transcription factors binding sites. Strong column: analysis with all CCVs at strong signals. ER-positive, ER-negative, ER-neutral: analysis of CCVs at strong signals stratified by phenotype.

enriched in T-47D active promoters. Conversely, CCVs were depleted among repressed gene-regulatory elements (defined by H3K27me3 marks) in normal breast (**Figure 3B**). As a control, we performed similar analyses with autoimmune disease CCVs ²⁹ (Methods) and relevant B and T cells (**Figures 3B-E**). The strongest evidence of enrichment of breast cancer CCVs was found at regulatory regions active in ER-positive cells (**Figure 3B**), whereas enrichment of autoimmune CCVs was in regulatory regions active in B and T cells (**Figure 3E**). We also compared the enrichment of our CCVs in enhancer-like and promoter-like regions (defined by ENCODE; **Supplementary Figure 1B**). The strongest evidence of enrichment of ER-positive CCVs in enhancer-like regions was found in MCF-7 cells, the only ER-positive cell line in ENCODE (**Supplementary Figure 1B**). These results highlight both the tissue- and disease-specificity of these histone marked gene regulatory regions.

(iv) We observed significant enrichment of CCVs in the binding sites for 40 TFBSs determined by ChIP-Seq (**Figures 3F-H**). The majority of the experiments were performed in ER-positive cell lines (90 TFBSs, 20 with data in ER-negative cell lines, 76 in ER-positive cell lines, and 16 in normal breast). These TFBSs

overlap each other and histone marks of active regulatory regions (**Supplementary Figure 2**). Enrichment in five TFBSs (ESR1, FOXA1, GATA3, TCF7L2, E2F1) has been previously reported ^{2,30}. All 40 TFBSs were significantly enriched in ER-positive CCVs (**Figure 3F**), seven were also enriched in ER-negative CCVs and nine in ER-neutral CCVs (**Figures 3G-H**). ESR1, FOXA1, GATA3 and EP300 TFBSs were enriched in all CCV ER-subtypes. However, the enrichment for ESR1, FOXA1 or GATA3 was stronger for ER-positive CCVs than for ER-negative or ER-neutral.

CCVs significantly overlap consensus transcription factor binding motifs

We investigated whether CCVs were also enriched within consensus TF binding motifs by conducting a motif-search within active regulatory regions (ER-positive CCVs at H3K4me1 marks in MCF-7). We identified 30 motifs, from eight TF families, with enrichment in ER-positive CCVs (FDR 10%, **Supplementary Table 4A**) and a further five motifs depleted among ER-positive CCVs. To assess whether the motifs appeared more frequently than by chance at active regulatory regions overlapped by our ER-positive CCVs, we compared motif-presence in a set of randomized control sequences (Methods). Thirteen of 30 motifs were more frequent at active regulatory regions with ER-positive CCV enrichment; these included seven homeodomain motifs and two fork head factors (**Supplementary Table 4B**).

When we looked at the change in predicted binding affinity, 57 ER-positive signals (86%) included at least one CCV predicted to modify the binding affinity of the enriched TFBSs (≥ 2 -fold, **Supplementary Table 4C**). Forty-eight ER-positive signals (73%) had at least one CCV predicted to modify the binding

affinity >10-fold. This analysis validates previous reports of breast cancer causal variants that alter DNA binding affinity for FOXA1^{3,30}

Bayesian fine -mapping incorporating functional annotations and linkage disequilibrium

As an alternative statistical approach, we applied PAINTOR³¹ to the same 128 regions (**Figure 1**). In brief, PAINTOR integrates genetic association results, linkage disequilibrium (LD) structure, and enriched genomic features in an empirical Bayes framework and derives the posterior probability (PP) of each variant being causal, conditional on available data. We identified seven variants with high posterior probability (HPP $\geq 80\%$) of being causal for all breast cancer types and ten for the ER-positive subtype (**Table 1**); two of these had HPP > 80% for both ER-positive and all breast cancer types. These 15 HPP variants (HPPVs; $\geq 80\%$) were distributed across 13 regions. We also identified an additional 35 variants in 25 regions with HPP ($\geq 50\%$ and < 80%) for ER-positive, ER-negative, or overall breast cancer (**Figure 2G**).

Consistent with the CCV analysis, we found evidence that most regions contained multiple HPPVs; the sum of PP across all variants in a region (an estimate of the number of distinct causal variants in the region) was > 2.0 for 84/86 regions analyzed for overall breast cancer, with a maximum of 16.1 and a mean of 6.4. For ER-positive cancer, 46/47 regions had total PP > 2.0 (maximum 18.3, mean 6.5) and for ER-negative, 17/23 regions had total PP > 2.0 (maximum 9.1, mean 3.2).

Although for many regions we were not able to identify HPP variants, we were able to reduce the proportion of variants needed to account for 80% of the total PP in a region to under 5% for 65 regions

for overall, 43 for ER-positive, and 18 for ER-negative breast cancer (**Figures S3A-C**). PAINTOR analyses were also able to reduce the set of likely causal variants in many cases. After summing the PPs for CCVs in each of the overall breast cancer signals, 39/100 strong-evidence signals had a total PP > 1.0. The number of CCVs in these signals ranged from 1 to 375 (median 24), but the number of variants needed to capture 95% of the total PP in each signal ranged from 1 to 115 (median 12), representing an average reduction of 43% in the number of variants needed to capture the signal.

PAINTOR and CCV analyses were generally consistent, yet complementary. Only 3.3% of variants outside of the set of strong-signal CCVs for overall breast cancer had PP > 1%, and only 48 (0.013%) of these had PP > 30% (**Supplementary Figure 3D**). At ER-positive and ER-negative signals respectively, 3.1% and 1.6% of the non-CCVs at strong signals had PP > 1%, and 40 (0.019%) and 3 (0.003%) of these had PP > 30% (**Figures S3E-F**). For the non-CCVs at strong-evidence signals with PP > 30%, the relatively high PP may be driven by the addition of functional annotation. The incorporation of functional annotation (relative to a PAINTOR model with no functional annotation) more than doubled PP for 64/88 variants.

CCVs co-localize with variants controlling local gene expression

We used four breast-specific expression quantitative trait loci (eQTL) data sets; to identify variants associated with differences in gene expression (eVariants): tumor tissue from the Nurses' Health Study (NHS) ³² and The Cancer Genome Atlas (TCGA) ³³, and normal breast tissue from the NHS and the Molecular Taxonomy of Breast Cancer International Consortium (METABRIC) ³⁴. We then examined the overlap of eVariants (defined as an eVariant within two orders of magnitude of the most significant

eVariant for a particular gene) with CCVs (Methods). There was significant overlap of CCVs with eVariants from both the NHS normal and breast cancer tissue studies (normal breast OR = 2.70, p-value = 1.7×10^{-5} ; tumor tissue OR = 2.34, p-value = 2.6×10^{-4} ; **Supplementary Table 3**). ER-neutral CCVs overlapped with eVariants in normal tissue more frequently than did ER-positive and ER-negative CCVs ($OR_{ER-neutral} = 3.51$, p-value = 1.3×10^{-5}). Cancer risk CCVs overlapped credible eVariants in 128/205 (62%) signals in at least one of the datasets (**Tables S5A-B**). Sixteen additional variants with PP $\geq 30\%$, not included among the CCVs, also overlapped with a credible eVariant (**Tables S5A-B**).

Transcription factors and known somatic breast cancer drivers are overrepresented among prioritized target genes

We assumed that causal variants function by affecting the behavior of a local target gene. However, it is challenging to define target genes or to determine how they may be affected by the causal variant. Few potentially causal variants directly affect protein coding: we observed 67/5,375 CCVs, and 19/137 HPPVs ($\geq 30\%$) in protein-coding regions. Of these, 33 (0.61%) were predicted to create a missense change, one a frameshift, and another a stop-gain, while 30 were synonymous (0.59%, **Supplementary Table 5C**). Four hundred and ninety-nine CCVs at 94 signals, and four additional HPPV ($\geq 30\%$), are predicted to create new splice sites or activate cryptic splice sites in 126 genes (**Supplementary Table 5D**). These results are consistent with previous observations that majority of common susceptibility variants are regulatory.

We applied an updated version of our pipeline INQUISIT - integrated expression quantitative trait and *in-silico* prediction of GWAS targets)² to prioritize potential target genes from 5,375 CCVs in strong

signals and all 138 HPPVs ($\geq 30\%$; **Supplementary Table 2C**). The pipeline predicted 1,204 target genes from 124/128 genomic regions examined. As a validation we examined the overlap between INQUISIT predictions and 278 established breast cancer driver genes³⁵⁻³⁹. Cancer driver genes were over-represented among high confidence (Level 1) targets; a 6-fold increase over expected from CCVs and 16-fold from HPPVs; $p\text{-value} = 1 \times 10^{-6}$; **Supplementary Figure 4A**). Notably, ten cancer driver genes (*CCND1*, *CHEK2*, *ESR1*, *FGFR2*, *GATA3*, *MAP3K1*, *MYC*, *TBX3*, *XPB1* and *ZFP36L1*) were predicted from the HPPVs derived from PAINTOR. Cancer driver gene status was consequently included as an additional weighting factor in the INQUISIT pipeline. TF genes⁴⁰ were also enriched amongst high-confidence targets predicted from both CCVs (2-fold, $p\text{-value} = 4 \times 10^{-4}$) and HPPVs (3-fold, $p\text{-value} = 7 \times 10^{-3}$, **Supplementary Figure 4A**).

In total INQUISIT prioritized 178 high-confidence target genes (**Table 2**, **Supplementary Table 6**). Significantly more genes were targeted by multiple independent signals ($N = 165$) than expected by chance ($p\text{-value} = 4.6 \times 10^{-8}$, **Supplementary Figure 4B**, **Figure 4A**). Six high-confidence predictions came only from HPPVs, although three of these (*IGFBP5*, *POMGNT1* and *WDYHV1*) had been predicted at lower confidence from CCVs. Target genes included 20 that were prioritized via potential coding/splicing changes (**Supplementary Table 7**), nine via promoter variants (**Supplementary Table 8**), and 166 via distal regulatory variants (**Supplementary Table 9**). We illustrate genes prioritized via multiple lines of evidence in **Figure 4A**.

Three examples of INQUISIT using genomic features to identify predict target genes. Based on capture Hi-C and ChIA-PET chromatin interaction data, *NR1P1* is a predicted target of intergenic CCVs and HPPVs

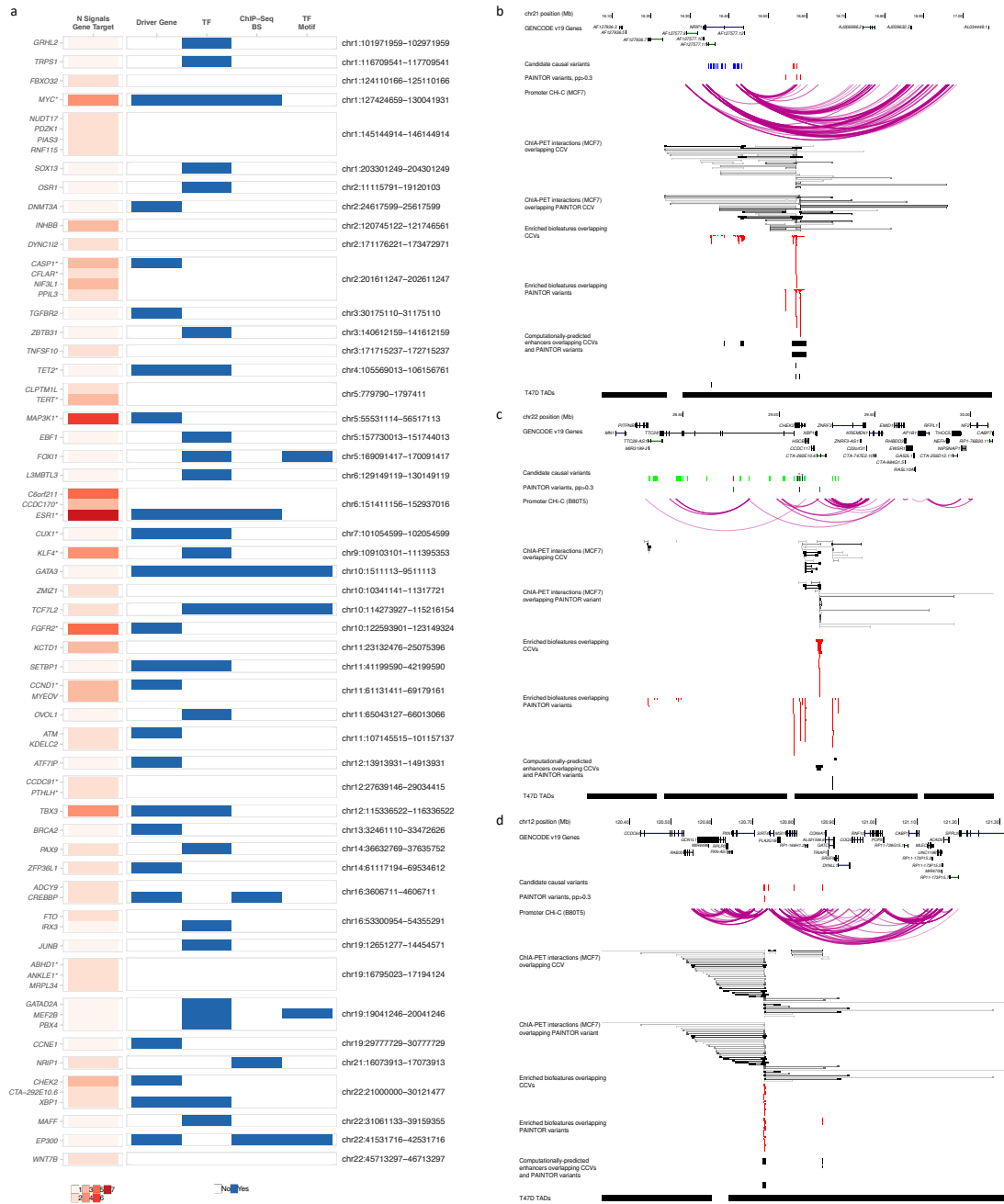


Figure 4. Predicted target genes are enriched in known breast cancer driver genes and transcription factors. (a) 79 target genes that fulfil at least one of the following criteria: are targeted by more than one independent signal, are known driver genes, transcription factor genes, or their binding sites (ChIP-Seq BS) or consensus motif (TF Motif) are significantly overlapped by CCVs. *Genes with published functional follow up. (b-d) In each panel, CCVs and PAINITOR variants with posterior probability >0.3 are shown, with independent signals in different colors. Chromatin interactions are shown as arcs (Capture Hi-C from selected breast cell lines) or boxes connected by lines, colored with gray-scale according to

interaction score (ENCODE ChIA-PET). Biofeatures which overlap CCVs from the global genomic enrichment analysis are depicted as red boxes. Computationally predicted enhancers including PreSTIGE, FANTOM5 and super-enhancers which overlap risk variants are represented by black boxes. High confidence INQUISIT target gene predictions include *NRIP1* (b), *CHEK2* and *XBP1* (c), and *RPLP0* and *MSI1* (d).

at chr21q21 (**Figure 4B**). Multiple target genes were predicted at chr22q12, including the driver genes *CHEK2* and *XBP1* (**Figure 4C**). A third example at chr12q24.31 is a more complicated scenario with two Level 1 targets: *RPLP0*⁴¹ and a modulator of mammary progenitor cell expansion, *MSI1*⁴² (Figure 4D).

Target gene pathways include DNA integrity-checkpoint, apoptosis, developmental processes and the immune system

We performed pathway analysis to identify common processes using INQUISIT high confidence target protein-coding genes (**Figure 5A**) and identified 457 Gene Ontology (GO) terms and 265 pathways at an FDR of 5% (**Supplementary Table 10**). These were grouped into 99 themes by common ancestor GO terms, pathways, or TF classes (**Figure 5B**). We found that 24% (14/58) of the ER-positive target genes were classified within developmental process pathways (including mammary development), 17% in immune system and a further 16% in cell differentiation pathways. Of genes targeted by ER-neutral signals, 19% (16/85) were classified in developmental process pathways, 18% in apoptotic process, and a further 16% in immune system pathways. The top themes of genes targeted by ER-negative signals were DNA integrity checkpoint (20%, 7/35), immune system, response to stimulus, and apoptotic processes, each containing 17% (6/35) of the genes.

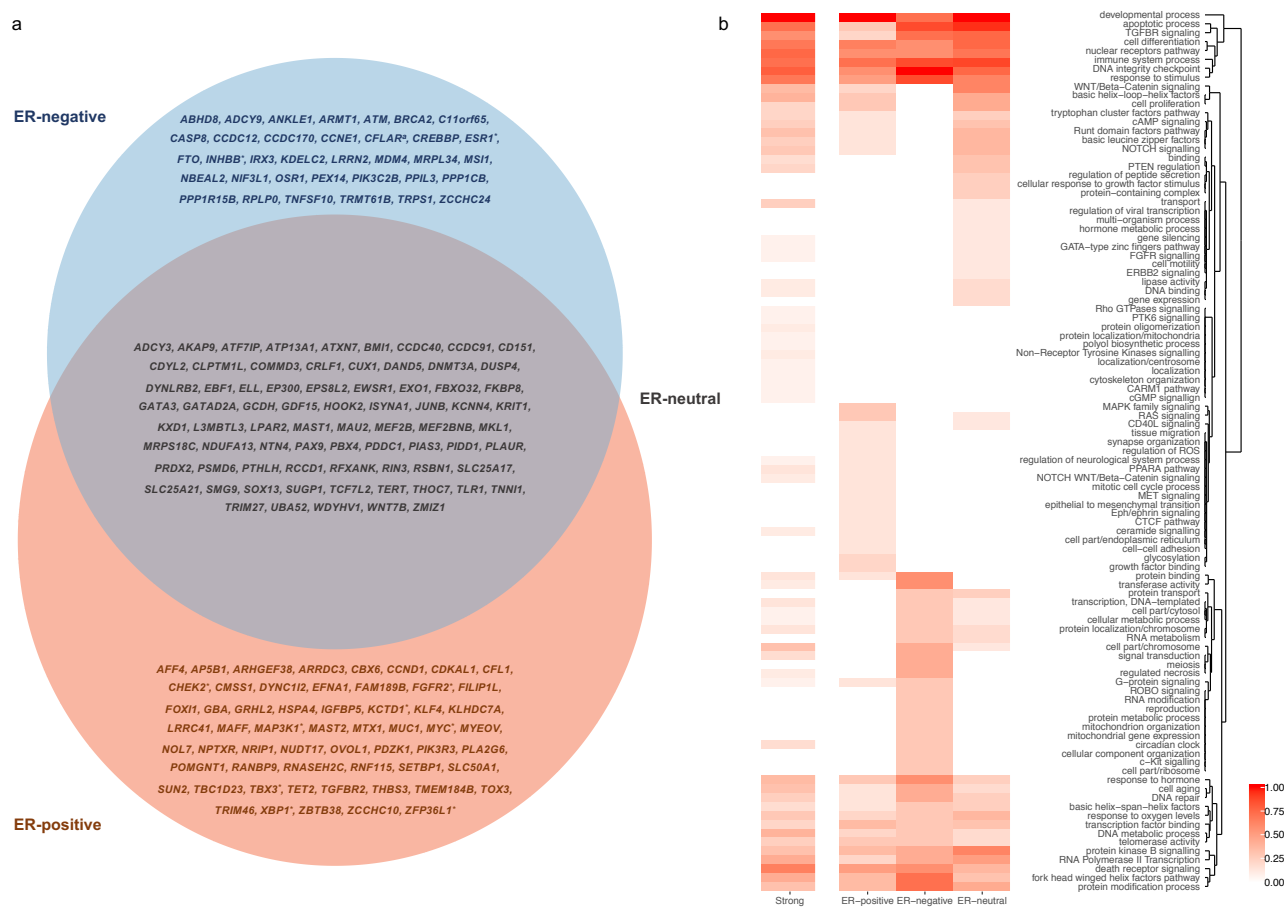


Figure 5. Predicted target genes by phenotype and significantly enriched pathways. (a) Venn diagram showing the associated phenotype (ER-positive, ER-negative, ER-neutral) for the Level 1 target genes, predicted by the CCVs and HPPVs. * ER-positive or ER-negative target genes also targeted by ER-neutral signals. (b) Heatmap showing clustering of pathway themes over-represented by INQUISIT Level 1 target genes. Color represents the relative number of genes per phenotype within enriched pathways, grouped by common themes. ER-positive, ER-negative, ER-neutral, and all phenotypes together (strong).

Novel pathways revealed by this study include TNF-related apoptosis-inducing ligand (TRAIL) signaling, the AP-2 transcription factors pathway, and regulation of I κ B kinase/NF- κ B signaling. Of note, the latter of these is specifically over-represented among ER-negative target genes. We also found significant

overrepresentation of additional carcinogenesis-linked pathways including cAMP, NOTCH, PI3K, RAS, WNT/Beta-catenin, and of receptor tyrosine kinases signaling, including FGFR, ERBB, or TGFBR⁴³⁻⁴⁷. Also of note, our target genes are significantly overrepresented in DNA damage checkpoint, DNA repair pathways, as well as programmed cell death pathways, such as apoptotic process, regulated necrosis, and death receptor signaling-related pathways.

DISCUSSION

We have performed multiple, complementary analyses on 150 breast cancer associated regions, originally found by GWAS, and identified 362 independent risk signals, 205 of these with high confidence (p-value < 10⁻⁶). We observed most regions contain multiple independent signals, the greatest number (nine) in the region surrounding *ESR1* and its co-regulated genes, and on 2q35, where *IGFBP5* appears to be a key target. We have used two complementary approaches to identify likely causal variants within each region: a Bayesian approach, PAINTOR, which integrated genetic associations, LD and informative genomic features, confirmed most associations found by the more traditional, multinomial regression approach, and also identified additional variants. Specifically, the Bayesian method highlighted 15 variants that are highly likely to be causal (HPP ≥ 80%). From these approaches we have identified a single variant, likely to be causal, at each of 34/205 signals (**Table 1**). Of these, only rs16991615 (*MCM8* p.E341K) and rs7153397 (*CCDC88C*, a cryptic splice-donor site) were predicted to affect protein-coding sequences. However, in other signals we also identified four coding changes previously recognized as deleterious, including the stop-gain rs11571833 (*BRCA2* p.K3326*, Meeks et al., 2016)⁴⁸ and two *CHEK2* coding variants; the frameshift rs555607708^{49,50}, and a missense variant, rs17879961^{51,52}. In addition, a splicing variant, rs10069690, in *TERT* results in the truncated

protein INS1b¹⁹, decreased telomerase activity, telomere shortening, and increased DNA damage response⁵³

Having identified potential causal variants within each signal, we aimed to uncover their functions at the DNA level and as well as trying to predict their target gene(s). Looking across all 150 regions, a notable feature is that many likely causal variants implicated in ER-positive cancer risk, lie in gene-regulatory regions marked as open and active in ER-positive breast cells, but not in other cell types. Moreover, a significant proportion of potential causal variants overlap the binding sites for transcription factor proteins (n=40 from ChIP-Seq) and co-regulators (n=64 with addition of computationally derived motifs). Furthermore, nine proteins also appear in the list of high-confidence target genes, hence the following genes and their products have been implicated by two different approaches: *CREBBP*, *EP300*, *ESR1*, *FOXI1*, *GATA3*, *MEF2B*, *MYC*, *NRIP1* and *TCF7L2*. Most of these proteins already have established roles in estrogen signaling. *CREBBP*, *EP300*, *ESR1*, *GATA3*, and *MYC* are also known cancer driver genes that are frequently somatically mutated in breast tumors.

In contrast to ER-positive signals, we identified fewer genomic features enriched in ER-negative signals. This may reflect the common molecular mechanisms underlying their development, but the power of this study was limited, despite including as many patients with ER-negative tumors as possible from the BCAC and CIMBA consortia. Less than 20% of genomic signals confer a greater risk of ER-negative cancer and there is little publicly available ChIP-Seq data on ER-negative breast cancer cell lines. The heterogeneity of ER-negative tumors may also have limited our power. Nevertheless, we have identified 35 target genes for ER-negative likely causal variants. Some of these already had functional

evidence supporting their role: including *CASP8*⁵⁴ and *MDM4*⁵⁵. Most targets, however, currently have no reported function in ER-negative breast cancer development.

Finally, we examined the gene-ontology pathways in which target genes most often lie. Of note, 12% (20/167) of all high-confidence target genes and 17% of ER-negative target predictions are in immune system pathways. Among the significantly enriched pathways were T cell activation, interleukin signaling, Toll-like receptor cascades, and I- κ B kinase/NF- κ B signaling, as well as processes leading to activation and perpetuation of the innate immune system. The link between immunity, inflammation and tumorigenesis has been extensively studied⁵⁶, although not primarily in the context of susceptibility. Four ER-negative high confidence target genes (*CASP8*, *CFLAR*, *ESR1*, *TNFSF10*) lie in the I- κ B kinase/NF- κ B signaling pathway. Interestingly, ER-negative cells have high levels of NF- κ B activity when compared to ER-positive⁵⁷. A recent expression–methylation analysis on breast cancer tumor tissue also identified clusters of genes correlated with DNA methylation levels, one enriched in ER signaling genes, and a second in immune pathway genes⁵⁸.

These analyses provide strong evidence for more than 200 independent breast cancer risk signals, identify the plausible cancer variants and define likely target genes for the majority of these. However, notwithstanding the enrichment of certain pathways and transcription factors, the biological basis underlying most of these signals remains poorly understood. Our analyses provide a rational basis for such future studies into the biology underlying breast cancer susceptibility.

METHODS

Study samples

Epidemiological data for European women were obtained from 75 breast cancer case-control studies participating in the Breast Cancer Association Consortium (BCAC) (cases: 40,285 iCOGS, 69,615 OncoArray; cases with ER status available: 29,561 iCOGS, 55,081 OncoArray); controls: 38,058 iCOGS, 50,879 OncoArray). Details of the participating studies, genotyping calling and quality control are given in ^{2,22,23}, respectively. Epidemiological data for *BRCA1* mutation carriers were obtained from 60 studies providing data to the Consortium of Investigators of Modifiers of *BRCA1* and *BRCA2* (CIMBA) (affected 1,591 iCOGS, 7,772 OncoArray; unaffected 1,665 iCOGS, 7,780 OncoArray). This dataset has been described in detail previously ^{1,59,60}. All studies provided samples of European ancestry. Any non-European samples were excluded from analyses.

Variant selection, genotyping and imputation

A dense set of variants surrounding susceptibility variants known at the time of design was selected for genotyping on the iCOGS array. To select markers for comprehensive interrogation of these densely-genotyped regions, all known variants from the March 2010 release of the 1000 Genomes Project with MAF > 0.02 in Europeans were identified, and all variants that were correlated with the published GWAS variants at $r^2 > 0.1$ together with a set of variants designed to tag all remaining variants at $r^2 > 0.9$ were selected. Twenty-one regions were densely genotyped with iCOGS (http://ccge.medschl.cam.ac.uk/files/2014/03/iCOGS_detailed_lists_ALL1.pdf). In total 26,978 iCOGS genotyped variants across the 152 mapped regions passed QC criteria. Similarly, all known associated risk variants at the time of the design of the OncoArray were included in the genotyping array. Variants

for fine-mapping were selected defining a 1Mb interval surrounding a known hit. Overlapping regions were merged into a single interval including 500kb either side of each lead signal. From among designable variants, all variants correlated with the known hits at $r^2 > 0.6$, all variants from lists of potentially functional variants, defined through RegulomeDB, and a set of variants designed to tag all remaining variants at $r^2 > 0.9$ were selected. Seventy-three regions were densely genotyped with OncoArray. In total 58,339 OncoArray genotyped variants across the 152 mapped regions passed QC criteria.

We imputed genotypes for the remaining variants at the genomic regions defined in the OncoArray design using IMPUTE2⁶¹, and the October 2014 release of the 1000 Genomes Project as a reference. To improve the accuracy at low frequency variants we used the standard IMPUTE2 MCMC algorithm for follow-up imputation (more detailed description of the parameters used can be found in²¹) We genotyped or successfully imputed 639,118 variants all having imputation info score ≥ 0.3 and minor allele frequencies (MAF) ≥ 0.001 in both the iCOGS and OncoArray datasets. Imputation summaries, and coverage for each of the analyzed regions stratified by allele frequency can be found in **Supplementary Table 1B**.

BCAC Statistical analyses

Per-allele odds ratios (OR) and standard errors (SE) were estimated for each variant using logistic regression. We ran this analysis separately for iCOGS and OncoArray, and separately for overall, ER-positive and ER-negative breast cancer. The association between each variant and breast cancer risk was adjusted by study (iCOGS) or country (OncoArray), and eight (iCOGS) or ten (OncoArray) ancestry-

informative principal components. The statistical significance for each variant was derived using a Wald test.

Defining the significance threshold

To establish an appropriate significance threshold for independent signals, all variants evaluated in the meta-analysis were included in logistic forward selection regression analyses for overall breast cancer risk in iCOGS cohort, run independently for each of the regions. We evaluated five p-value thresholds for inclusion: $< 1 \times 10^{-4}$, $< 1 \times 10^{-5}$, $< 1 \times 10^{-6}$, $< 1 \times 10^{-7}$, and $< 1 \times 10^{-8}$. The most parsimonious iCOGS models were tested in OncoArray, and the false discovery rate (FDR) at 1% level for each one of the thresholds was estimated using the Benjamini-Hochberg procedure⁶². At a 1% FDR threshold, 72% of variants of variants significant at $p < 10^{-4}$ replicated on the OncoArray, whereas 94% of variants significant at $p < 10^{-6}$ replicated. Based on these analyses, two categories were defined: strong-evidence signals (conditional p-values $< 10^{-6}$ when the signal is included in the final model fit using the inclusion threshold $p < 10^{-4}$), and moderate-evidence signals (conditional p-values $< 10^{-4}$ and $\geq 10^{-6}$ in the final model).

Identification of independent signals

To identify independent signals, we ran multinomial stepwise regression analyses, separately in iCOGS and OncoArray, for all the variants displaying evidence of association ($N_{\text{variants}} = 202,749$). We selected two sets of well imputed variants (imputation info score ≥ 0.3 in both iCOGS and OncoArray): (a) common and low frequency variants ($\text{MAF} \geq 0.01$) with a threshold for inclusion of logistic regression p-value ≤ 0.05 in either the iCOGS or OncoArray datasets for at least one of the three phenotypes: overall, ER-positive and ER-negative breast cancer; and (b) rarer variants ($\text{MAF} \geq 0.001$ and < 0.01), with a threshold for inclusion of a logistic regression p-value ≤ 0.0001 . The same parameters used for adjustment in logistic regression were used in the multinomial regression analysis (R function

multinom). The multinomial regression estimates were combined using a fixed-effects meta-analysis weighted by the inverse variance⁶³. Variants with the lowest conditional p-value from the meta-analysis of both European cohorts at each step were included into the multinomial regression model. However, if the new variant to be included in the model caused collinearity problems due to be highly correlated with an already selected variant, or showed high heterogeneity ($p\text{-value} < 10^{-4}$) between iCOGS and OncoArray after being conditioned by the variant(s) in the model; we dropped the new variant and repeated this process.

The main signal at 105 of 152 evaluated regions demonstrated genome-wide significance, while 44 were marginally significant ($9.89 \times 10^{-5} \geq p\text{-value} > 5 \times 10^{-8}$). For two regions there were no variants significant at $p < 10^{-4}$ (chr14:104712261-105712261; rs10623258 multinomial regression p-value = 2.32×10^{-4} ; chr19:10923703-11923703, rs322144, multinomial regression p-value = 3.90×10^{-3}). There are four main differences in the dataset used in the analysis and that used in the previous paper that account for these differences : (i) our previous paper² included data from 11 additional GWAS studies (14,910 cases and 17,588 controls) that have not been included in the present analysis in order to minimize differences in array coverage; (ii) the present analysis evaluated the risk of ER-positive and ER-negative disease concurrently, whereas in our previous paper the outcome was overall breast cancer risk. ER status was available for only 73% of the iCOGS and 79% of the OncoArray breast cancer cases (iii) for the set of samples genotyped with both arrays, ² included iCOGS genotypes, while this study includes OncoArray genotypes to maximize the number of samples genotyped with a larger coverage; and (iv) imputation parameters at fine mapping-regions were modified to improve the imputation accuracy of less frequent variants.

Selection of a credible set of variants candidates to be causal

Variants with p-values within two orders of magnitude of the top variant for each signal, after adjusting for the index variant of preceding signals, were considered as the credible set of candidates to drive the association at each independent signal (CCVs) ²⁴We defined the best model, among those including one CCVs for each signal, by iteratively conditioning on the selected CCVs in the other signals. For ten fine mapping regions (chr4:175328036-176346426, chr5:55531884-56587883, chr6:151418856-152937016, chr8:75730301-76917937, chr10:80341148-81387721, chr10:122593901-123849324, chr12:115336522-116336522, chr14:36632769-37635752, chr16:3606788-4606788, chr22:38068833-39859355) a model including the lowest conditioned p-value variants (index variant) at each signal could not be found. In that case we estimated the best model as the model with the largest chi-square, from all the possible combinations of credible variants. Variants in strong signals were conditioned by the additional strong confidence signals whereas variants for moderate confidence signals were conditioned by all the independent signals. We then redefined the credible set of candidate variants for each signal using the conditional p-values by the additional independent signals. Thus, variants with p-values within two orders of magnitude of the top variant for each signal, after adjusting for all the index variant of the additional signals at the locus, were considered as the final credible set of candidates.

Case -only analysis

Differences in the effect size between ER-positive and ER-negative disease for each index independent variant were assessed using a case-only analysis. We performed logistic regression with ER status as the

dependent variable, and the lead variant at each strong signal in the fine mapping region as the independent variables. We use FDR (5%) to adjust for multiple testing.

OncoArray-only stepwise analysis

To evaluate whether the lower coverage in iCOGS could affect the identification of independent signals, we ran stepwise multinomial regression using only the OncoArray dataset. We identified 249 independent signals. Ninety-two signals, in 67 fine mapping regions, achieved a genome-wide significance level (conditional p-value < 5×10^{-8}). Two hundred and five of these signals were also identified in the meta-analysis with iCOGS. Nine independent variants across ten regions were not evaluated in the combined analysis due to their low imputation info score in iCOGS. Out of these nine signals, two signals would be classified as main primary signals, rs114709821 at region chr1:145144984-146144984 (OncoArray imputation info score = 0.72), and rs540848673 at region chr1:149406413-150420734 (OncoArray imputation info score = 0.33). Given the low number of additional signals identified in the OncoArray dataset alone, all analyses were based on the combined iCOGS/OncoArray dataset.

CIMBA statistical analysis

CIMBA provided data from 60 retrospective cohort studies consisting of 9,445 unaffected and 9,363 affected female *BRCA1* mutation carriers of European ancestry. Unconditional (i.e. single variant) analyses were performed using a score test based on the retrospective likelihood of observing the genotype conditional on the disease phenotype^{64,65}. Conditional analyses, where more than one variant is analyzed simultaneously, cannot be performed in this score test framework. Therefore,

conditional analyses were performed by Cox regression, allowing for adjustment of the conditionally independent variants identified by the BCAC/DRIVE analyses. All models were stratified by country and birth cohort, and adjusted for relatedness (unconditional models used kinship adjusted standard errors based on the estimated kinship matrix; conditional models used cluster robust standard errors based on phenotypic family data).

Data from the iCOGS array and the OncoArray were analyzed separately and combined to give an overall *BRCA1* association by fixed-effects meta-analysis. Variants were excluded from further analyses if they exhibited evidence of heterogeneity (Heterogeneity p-value < 1×10^{-4}) between iCOGS and OncoArray, had MAF < 0.005, were poorly imputed (imputation info score < 0.3) or were imputed to iCOGS only (i.e. must have been imputed to OncoArray or iCOGS and OncoArray).

Meta-analysis of ER-negative cases in BCAC with *BRCA1* mutation carriers from CIMBA

BRCA1 mutation carrier association results were combined with the BCAC multinomial regression ER-negative association results in a fixed-effects meta-analysis. Variants considered for analysis must have passed all prior QC steps and have had $MAF \geq 0.005$. All meta-analyses were performed using the METAL software ⁶⁶. Instances where spurious associations might occur were investigated by assessing the LD between a possible spurious association and the conditionally independent variants. High LD between a variant and a conditionally independent variant within its region causes model instability through collinearity and the convergence of the model likelihood maximization may not be reliable. Where the association appeared to be driven by collinearity, the signals were excluded.

eQTL analysis

Total RNA was extracted from normal breast tissue in formalin-fixed paraffin embedded breast cancer tissue blocks from 264 Nurses' Health Study (NHS) participants ³². Transcript expression levels were measured using the Glue Grant Human Transcriptome Array version 3.0 at the Molecular Biology Core Facilities, Dana-Farber Cancer Institute. Gene expression was normalized and summarized into Log₂ values using RMA (Affymetrix Power Tools v1.18.012); quality control was performed using GlueQC and arrayQualityMetrics v3.24.014. Genome-wide data on variants were generated using the Illumina HumanHap 550 BeadChip as part of the Cancer Genetic Markers of Susceptibility initiative ⁶⁷. Imputation to the 1000KGP Phase 3 v5 ALL reference panel was performed using MACH to pre-phase measured genotypes and minimac to impute.

Expression analyses were performed using data from The Cancer Genome Atlas (TCGA) and Molecular Taxonomy of Breast Cancer International Consortium (METABRIC) projects ^{34,38}. The TCGA eQTL analysis was based on 458 breast tumors that had matched gene expression, copy number and methylation profiles together with the corresponding germline genotypes available. All 458 individuals were of European ancestry as ascertained using the genotype data and the Local Ancestry in admixed Populations (LAMP) software package (LAMP estimate cut-off >95% European)⁶⁸. Germline genotypes were imputed into the 1000 Genomes Project reference panel (October 2014 release) using IMPUTE version 2 ^{69,70}. Gene expression had been measured on the Illumina HiSeq 2000 RNA-Seq platform (gene-level RSEM normalized counts ⁷¹), copy-number estimates were derived from the Affymetrix SNP 6.0 (somatic copy-number alteration minus germline copy-number variation called using the GISTIC2 algorithm ⁷²), and methylation beta values measured on the Illumina Infinium HumanMethylation450.

Expression QTL analysis focused on all variants within each of the 152 genomic intervals that had been subjected to fine-mapping for their association with breast cancer susceptibility. Each of these variants was evaluated for its association with the expression of every gene within 2 Mb that had been profiled for each of the three data types. The effects of tumor copy number and methylation on gene expression were first regressed out using a method described previously⁷³. eQTL analysis was performed by linear regression, with residual gene expression as outcome, germline SNP genotype dosage as the covariate of interest and ESR1 expression and age as additional covariates, using the R package Matrix eQTL⁷⁴.

The METABRIC eQTL analysis was based on 138 normal breast tissue samples resected from breast cancer patients of European ancestry. Germline genotyping for the METABRIC study was also done on the Affymetrix SNP 6.0 array, and gene expression in the METABRIC study was measured using the Illumina HT12 microarray platform (probe-level estimates). No adjustment was implemented for somatic copy number and methylation status since we were evaluating eQTLs in normal breast tissue. All other steps were identical to the TCGA eQTL analysis described above.

Genomic feature enrichment

We explored the overlap of candidate and excluded variants with 90 transcription factors, 10 histone marks, and DNase hypersensitivity sites in 15 breast cell lines, and eight normal human breast tissues. We analysed data from the Encyclopedia of DNA Elements (ENCODE) Project^{75,76}, Roadmap Epigenomics Projects⁷⁷, the International Human Epigenome Consortium^{78, 27, 79}, The Cancer Genome Atlas (TCGA)³³, the Molecular Taxonomy of Breast Cancer International Consortium (METABRIC)³⁴, ReMap database (We included 241 TF annotations from ReMap (of 2825 total) which

showed at least 2% overlap for any of the phenotype SNP sets)⁸⁰, and other data obtained through the National Center for Biotechnology Information (NCBI) Gene Expression Omnibus (GEO). Promoters were defined following the procedure defined in Pellacani et al.⁷⁹, that is +/- 2Kb from a gene transcription start site, using an updated version of the RefSeq genes (refGene, version updated 2017-04-11)⁸¹. Transcribed regions were defined using the same version of refSeq genes. lncRNA annotation was obtained from GENCODE (v19)⁸²

To include eQTL results in the enrichment analysis we (i) identified all the genes for which summary statistics were available, for each study; (ii) defined the most significant eQTL variant for each gene (index eQTL variant, p-value threshold $\leq 5 \times 10^{-4}$); (iii) classified variants with p-values within two orders of magnitude of the index eVariant as the credible set of eQTL variants candidate to drive the expression of the gene. Those variants part of at least one eQTL credible set were defined as eVariants. We evaluated the overlap between eQTL credible sets and CCVs (risk variants credible set). We evaluated the enrichment of CCVs for genomic feature using logistic regression, with CCV (vs non-CCV variants) being the outcome. To adjust for the correlation among variants in the same fine mapping region, we used robust variance estimation for clustered observations (R function *multiwaycov*). The associated variants at FDR 5% were included into a stepwise forward logistic regression procedure to select the most parsimonious model. A likelihood ratio test was used to compare multinomial logistic regression models with and without equality effect constraints to evaluate whether there was heterogeneity among the effect sizes for ER-positive, ER-negative or signals equally associated with both phenotypes (ER-neutral).

To validate the disease specificity of the regulatory regions identified through this analysis we follow the same approach for the autoimmune related CCVs from ²⁹ (N = 4,192). Variants excluded as candidate causal variants, and within 500 kb upstream and downstream of the index variant for each signal were classified as excluded variants (N = 1,686,484). We then tested the enrichment for both the breast cancer and autoimmune CCVs with breast and T and B cell enhancers. We also evaluated the overlap of our CCVs with ENCODE enhancer-like and promoter-like regions for 111 tissues, primary cells, immortalized cell line, and in vitro differentiated cells. Of these, 73 had available data for both enhancer- and promoter-like regions.

Transcription binding site motif analysis

We conducted a search to find motif occurrences for the transcription factors significantly enriched in the genomic featured. For this we used two publicly available databases, Factorbook ⁸³ and JASPAR 2016 ⁸⁴. For the search using Factorbook we included the motifs for the transcription factors discovered in the cell lines where a significant enrichment was found in our genomic features analysis. We also searched for all the available motifs for *Homo sapiens* at the JASPAR database (*JASPAR CORE 2016, TFBSTools* ⁸⁵) Using as reference the USCS sequence (*BSgenome.Hsapiens.USCS.hg19*) we created fasta sequences with the reference and alternative alleles for all the variants included in our analysis plus 20 bp flanking each variant. We used FIMO (version 4.11.2, Grant et al., 2011) ⁸⁶ to scan all the fasta sequences searching for the JASPAR and Factorbook motifs to identify any overlap of any of the alleles for each of the variants (setting the p-value threshold to 10^{-3}). We subsequently determined whether our CCVs were more frequency overlapping a particular TF binding motif when compared with the excluded variants. We ran these analyses for all the strong signals, but also strong signals stratified by

ER status. Also, we subset this analysis to the variants located at regulatory regions in an ER-positive cell line (MCF-7 marked by H3K4me1, ENCODE id: ENCFF674BKS) and evaluated whether the ER-positive CCVs overlap any of the motifs more frequently than the excluded variants. We also evaluated the change in total binding affinity caused by the ER-positive CCCR alternative allele for all but one (2:217955891:T:<CN0>:0) of the ER-positive CCVs (*MatrixRider*⁸⁷).

Subsequently, we evaluated whether the MCF-7 regions demarked by H3K4me1 (ENCODE id: ENCFF674BKS), and overlapped by ER-positive CCVs, were enriched in known TFBS motifs. We first subset the ENCODE bed file ENCFF674BKS to identify MCF-7 H3K4me1 peaks overlapped by the ER-positive CCVs (N = 107), as well as peaks only overlapped by excluded variants (N = 11,099), using BEDTools⁸⁸. We created fasta format sequences using genomic coordinate data from the intersected bed files. In order to create a control sequence set, we used the script included with the MEME Suite (*fasta-shuffle-letters*) to create 10 shuffled copies of each sequence overlapped by ER-positive CCVs (N = 1,070). We then used AME⁸⁹ to interrogate whether the 107 MCF-7 H3K4me1 genomic regions overlapped by ER-positive CCVs were enriched in known TFBS consensus motifs when compared to the shuffled control sequences, or to the MCF-7 H3K4me1 genomic regions overlapped only by excluded variants. We used the command line version of AME (version 4.12.0) selecting as scoring method the total number of positions in the sequence whose motif score p-value is less than 10^{-3} , and using a one-tailed Fisher's Exact test as the association test.

PAINTOR analysis

To further refine the set of CCVs, we performed empirical Bayes fine-mapping using PAINTOR to integrate marginal genetic association summary statistics, linkage disequilibrium patterns, and biological features^{31,90}. PAINTOR places higher prior probability for causality on variants that fall in particular genomic features and learns the priors for different genomic features from the aggregate association results across all of the regions being mapped. PAINTOR does not assume a fixed number of causal variants in each region, although it implicitly penalizes non-parsimonious causal models. We applied PAINTOR separately to association results for overall breast cancer (in 85 regions determined to have at least one ER-neutral association or ER-positive and ER-negative association), ER-positive breast cancer (in 48 regions determined to have at least one ER-positive-specific association), and ER-negative breast cancer (in 22 regions determined to have at least one ER-negative-specific association). To avoid artifacts due to mis-matches between the LD in study samples and the LD matrix supplied to PAINTOR, we used association logistic regression summary statistics from OncoArray data only and estimated the LD structure in the OncoArray sample. For each endpoint we fit four models with increasing numbers of genomic features selected from the stepwise enrichment analyses described above: Model 0 (with no genomic features—assumes each variant is equally likely to be causal a priori), Model 1 (with those genomic features selected with stopping rule $p < 0.001$); Model 2 (with those genomic features selected with stopping rule $p < 0.01$); and Model 3 (with those genomic features selected with stopping rule $p < 0.05$).

We used the Bayesian Information Criterion (BIC) to choose the best-fitting model for each outcome. As PAINTOR estimates the marginal log likelihood of the observed Z scores using Gibbs sampling, we used a shrunk mean BIC across multiple Gibbs chains to account for the stochasticity in the log-

likelihood estimates. We ran PAINTOR four times to generate four independent Gibbs chains estimated the BIC difference between model i and model j as $\Delta_{ij} = \left(\frac{100}{V+100}\right)(BIC_i - BIC_j)$. This assumes a $N(0,100)$ prior on the difference, or roughly a 16% chance that model i would be decisively better than model j (i.e. $|BIC_i - BIC_j| > 10$). We then proceeded to choose the best-fitting model in a stepwise fashion: starting with a model with no annotations, we selected a model with more annotations in favor a model with fewer if the larger model was a considerably better fit—i.e. $\Delta_{ij} > 2$. Model 1 was the best fit according to this process for overall and ER-positive breast cancer; Model 0 was the best fit for ER-negative breast cancer.

Differences between the PAINTOR and CCV outputs may be due to several factors. By considering functional enrichment and joint LD among all SNPs, PAINTOR may refine the set of likely causal variants; rather than imposing a hard threshold, PAINTOR allows for a gradient of evidence supporting causality; and the two sets of calculations are based on different summary statistics, CCV analyses used both iCOGS and OncoArray genotypes, while PAINTOR used only OncoArray data (**Figure 1**, Methods).

Variant annotation

Variants genome coordinates were converted to assembly GRCh38 with liftOver and uploaded to Variant Effect Predictor ⁹¹ to determine their effect on genes, transcripts, and protein sequence. The commercial software Alamut[®] Batch v1.6 batch was also used to annotate coding and splicing variants. PolyPhen-2 ⁹², SIFT ⁹³, MAPP ⁹⁴ were used to predict the consequence of missense coding variants. MaxEntScan ⁹⁵, Splice-Site Finder, and Human Splicing Finder ⁹⁶ were used to predict splicing effects.

INQUISIT analysis

Logic underlying INQUISIT predictions

Briefly, genes were considered to potential targets of risk variants when variants affect: (1) distal regulation, (2) proximal genomic information, including chromatin interactions from capture Hi-C experiments performed in a panel of six breast cell lines ⁹⁷, chromatin interaction analysis by paired-end tag sequencing (ChIA-PET; ⁹⁸) and genome-wide chromosome conformation capture from HMECs (Hi-C, (Rao et al., 2014)). We used computational enhancer–promoter correlations (PreSTIGE ⁹⁹, IM-PET (He et al., 2014), FANTOM5 ¹⁰⁰ and super-enhancers ²⁸), results for breast tissue-specific expression variants (eVariants) from multiple independent studies (TCGA, METABRIC, NHS, Methods), allele-specific imbalance in gene expression ¹⁰¹, transcription factor and histone modification chromatin immunoprecipitation followed by sequencing (ChIP-Seq) from the ENCODE and Roadmap Epigenomics Projects together with the genomic features found to be significantly enriched as described above, gene expression RNA-seq from several breast cancer lines and normal samples and topologically associated domain (TAD) boundaries from T47D cells (ENCODE, ¹⁰², Methods and Key Resources Table). To assess the impact of intragenic variants, we evaluated their potential to alter splicing using Alamut® Batch to identify new and cryptic donors and acceptors, and several tools to predict effects of coding sequence changes (Methods). The output from each tool was converted to a binary measure to indicate deleterious or tolerated predictions.

Scoring hierarchy

Each target gene prediction category (distal, promoter or coding) was scored according to different criteria. Genes predicted to be distally-regulated targets of CCVs were awarded points based on physical

links (eg ChI-C), computational prediction methods, allele-specific expression, or eVariant associations. All CCV and HPPVs were considered as potentially involved in distal regulation. Intersection of a putative distal enhancer with genomic features found to be significantly enriched (see '**Genomic features enrichment**' for details) were further upweighted. CCVs and HPPVs in gene proximal regulatory regions were intersected with histone ChIP-Seq peaks characteristic of promoters and assigned to the overlapping transcription start sites (defined as -1.0 kb - +0.1 kb). Further points were awarded to such genes if there was evidence for eVariant association or allele-specific expression, while a lack of expression resulted in down-weighting as potential targets. Potential coding changes including missense, nonsense and predicted splicing alterations resulted in addition of one point to the encoded gene for each type of change, while lack of expression reduced the score. We added an additional point for predicted target genes that were also breast cancer drivers. For each category, scores ranged from 0-7 (distal); 0-3 (promoter) or 0-2 (coding). We converted these scores into 'confidence levels': Level 1 (highest confidence) when distal score > 4, promoter score ≥ 3 or coding score > 1; Level 2 when distal score ≤ 4 and ≥ 1 , promoter score = 1 or = 2, coding score = 1; and Level 3 when distal score < 1 and > 0, promoter score < 1 and > 0, and coding < 1 and > 0. For genes with multiple scores (for example, predicted as targets from multiple independent risk signals or predicted to be impacted in several categories), we recorded the highest score. Driver and transcription factor gene enrichment analysis was carried out using INQUISIT scores prior to adding a point for driver gene status. Modifications to the pipeline since original publication ² include:

- TAD boundary definitions from ENCODE T47D Hi-C analysis. Previously, we used regions from Rao, Cell 2013;
- eQTL: Addition of NHS normal and tumor samples

- allele-specific imbalance using TCGA and GTEx RNA-seq data ¹⁰¹
- Capture Hi-C data from six breast cell lines (Beesley et al.)
- Additional biofeatures derived from global enrichment in this study.

Multi-signal targets

To test if more genes were targeted by multiple signals than expected by chance, we modelled the number of signals per gene by negative binomial regression (R function *glm.nb*, package MASS) and Poisson regression (R function *glm*, package stats) with ChIA-PET interactions as a covariate and adjusted by fine mapping region. Likelihood ratio tests were used to compare goodness of fit. Rootograms were created using the R function *rootogram* (package vcd).

Pathway analysis

The pathway gene set database, dated 1 September 2018 was used ¹⁰³ (http://download.baderlab.org/EM_Genesets/current_release/Human/symbol/). This database contains pathways from Reactome ¹⁰⁴, NCI Pathway Interaction Database ¹⁰⁵, GO (Gene Ontology) ¹⁰⁶, HumanCyc ¹⁰⁷, MSigdb ¹⁰⁸, NetPath ¹⁰⁹, and Panther ¹¹⁰. All duplicated pathways, defined in two or more databases, were included. To provide more biologically meaningful results, only pathways that contained ≤ 200 genes were used.

We interrogated the pathway annotation sets with the list of high-confidence (Level 1) INQUISIT gene list. The significance of over-representation of the INQUISIT genes within each pathway was assessed with a hypergeometric test, ¹¹¹, using the R function *phyper* as follows:

$$P(x|n, m, N) = 1 - \sum_{i=0}^{x-1} \frac{\binom{m}{i} \binom{N-m}{n-i}}{\binom{N}{n}}$$

where x is the number of Level 1 genes that overlap with any of the genes in the pathway, n is the number of genes in the pathway, m is the number of Level1 genes that overlap with any of the genes in the pathway data set ($m_{\text{strong GO}} = 135$, $m_{\text{ER-positive GO}} = 48$, $m_{\text{ER-negative GO}} = 26$, $m_{\text{ER-neutral GO}} = 73$; $m_{\text{strong Pathways}} = 114$, $m_{\text{ER-positive Pathways}} = 36$, $m_{\text{ER-negative Pathways}} = 21$, $m_{\text{ER-neutral Pathways}} = 67$), and N is the number of genes in the pathway data set ($N_{\text{Genes GO}} = 14,252$, $N_{\text{Genes Pathways}} = 10,915$). We only included pathways that overlapped with at least two Level 1 genes. We used the Benjamini-Hochberg false discovery rate (FDR) ⁶² at 5% level.

ACKNOWLEDGMENTS

We thank all the individuals who took part in these studies and all the researchers, clinicians, technicians and administrative staff who have enabled this work to be carried out. This work was supported by the European Union's Horizon 2020 research and innovation programme under the Marie Skłodowska-Curie grant agreement No 656144. Genotyping of the OncoArray was principally funded from three sources: the PERSPECTIVE project, funded by the Government of Canada through Genome Canada and the Canadian Institutes of Health Research, the 'Ministère de l'Économie, de la Science et de l'Innovation du Québec' through Genome Québec, and the Quebec Breast Cancer Foundation; the NCI Genetic Associations and Mechanisms in Oncology (GAME-ON) initiative and Discovery, Biology and Risk of Inherited Variants in Breast Cancer (DRIVE) project (NIH Grants U19 CA148065 and X01HG007492); and Cancer Research UK (C1287/A10118 and C1287/A16563). BCAC is funded by

Cancer Research UK (C1287/A16563), by the European Community's Seventh Framework Programme under grant agreement 223175 (HEALTH-F2-2009-223175) (COGS) and by the European Union's Horizon 2020 Research and Innovation Programme under grant agreements 633784 (B-CAST) and 634935 (BRIDGES). Genotyping of the iCOGS array was funded by the European Union (HEALTH-F2-2009-223175), Cancer Research UK (C1287/A10710), the Canadian Institutes of Health Research for the 'CIHR Team in Familial Risks of Breast Cancer' program, and the Ministry of Economic Development, Innovation and Export Trade of Quebec, grant PSR-SIIRI-701. Combining of the GWAS data was supported in part by The National Institute of Health (NIH) Cancer Post-Cancer GWAS initiative grant U19 CA 148065 (DRIVE, part of the GAME-ON initiative). For a full description of funding and acknowledgments, see Supplementary Note.

AUTHOR CONTRIBUTIONS

Conceptualization: L.Fa., H.As., J.Be., D.R.B., J.Al., S.Ka., K.A.P., K.Mi., P.So., A.Le., M.Gh., P.D.P.P., J.C.C., M.G.C., M.K.S., R.L.M., V.N.K., J.D.E., S.L.E., A.C.A., G.C.T., J.Si., D.F.E., P.K., A.M.D. Methodology: L.Fa., H.As., J.Be., D.R.B., J.Al., J.D.E., S.L.E., A.C.A., G.C.T., J.Si., D.F.E., P.K., A.M.D. Software: J.Be., J.P.T., M.L. Formal analysis: L.Fa., H.As., J.Be., D.R.B., J.Al., S.Ka., C.Tu., M.Mor., X.J. Resources: S.A., K.A., M.R.A., I.L.A., H.A.C., N.N.A., A.A., V.A., K.J.A., B.K.A., B.A., P.L.A., J.Az., J.Ba., R.B.B., D.B., A.B.F., J.Ben., M.B., K.B., A.M.B., C.B., W.B., N.V.B., S.E.B., B.Bo., A.B., H.Bra., H.Bre., I.B., I.W.B., A.B.W., T.B., B.Bu., S.S.B., Q.C., T.C., M.A.C., N.J.C., I.C., F.C., J.S.C., B.D.C., J.E.C., J.C., H.C., W.K.C., K.B.M., C.L.C., J.M.C., S.C., F.J.C., A.C., S.S.C., C.C., K.C., M.B.D., M.D.H., P.D., O.D., Y.C.D., G.S.D., S.M.D., T.D., I.D.S., A.D., S.D., M.Dum., M.Dur., L.D., M.Dw., D.M.E., C.E., M.E., D.G.E., P.A.F., U.F., O.F., G.F., H.F., L.Fo., W.D.F., E.F., L.Fr., D.F., M.Ga., M.G.D., G.Ga., P.A.G., S.M.G., J.Ga., J.A.G., M.M.G., V.G., G.G.G., G.Gl., A.K.G., M.S.G., D.E.G.,

A.G.N., M.H.G., M.Gr., J.Gr., A.G., P.G., E.H., C.A.H., N.H., P.Ha., U.H., P.A.H., J.M.H., M.H., W.H., C.S.H., B.A.M., J.H., P.Hi., F.B.L., A.H., M.J.H., J.L.H., A.Ho., G.H., P.J.H., E.N.I., C.I., M.I., A.Jag., M.J., A.Jak., P.J., R.J., R.C.J., E.M.J., N.J., M.E.J., A.Juk., A.Jun., R.Ka., D.K., B.Pes., R.Ke., M.J.K., E.K., J.I.K., J.K., C.M.K., Y.K., I.K., V.K., S.Ko., K.K.S., T.K., A.K., K.K., Y.L., D.L., E.L., G.L., J.Le., F.L., A.Li., W.L., J.Lo., A.Lo., J.T.L., J.Lu., R.J.M., T.M., E.M., A.Ma., M.Ma., S.Man., S.Mag., M.E.M., K.Ma., D.M., R.M., L.M., C.M., N.Me., A.Me., P.M., A.Mi., N.Mi., M.Mo., F.M., A.M.M., V.M.M., T.A., S.A.N., R.N., K.L.N., N.Z.N., H.N., P.N., F.C.N., L.N.Z., A.N., K.O., E.O., O.I.O., H.O., N.O., A.O., V.S.P., J.Pa., S.K.P., T.W.P.S., M.T.P., J.Pau., I.S.P., B.Pei., B.Y.K., P.P., J.Pe., D.P.K., K.Pr., R.P., N.P., D.P., M.A.P., K.Py., P.R., S.J.R., J.R., R.R.M., G.R., H.A.R., M.R., A.R., C.M.R., E.S., E.S.H., D.P.S., M.Sa., C.Sa., E.J.S., M.T.S., D.F.S., R.K.S., A.S., M.J.S., B.S., P.Sc., C.Sc., R.J.S., L.S., C.M.D., M.Sh., P.Sh., C.Y.S., X.S., C.F.S., T.P.S., S.S., M.C.S., J.J.S., A.B.S., J.St., D.S.L., C.Su., A.J.S., R.M.T., Y.Y.T., W.J.T., J.A.T., M.R.T., M.Te., S.H., M.B.T., A.T., M.Th., D.L.T., M.G.T., M.Ti., A.E.T., R.A.E., I.T., D.T., G.T.M., M.A.T., N.T., M.Tz., H.U.U., C.M.V., C.J.A., L.E.K., E.J.R., A.Ve., A.Vi., J.V., M.J.V., Q.W., B.W., C.R.W., J.N.W., C.W., H.W., R.W., A.W., A.H.W., D.Y., Y.Z., W.Z. Data management and curation: K.Mi., J.D., M.K.B., Q.W., R.Ke., J.C.C. and M.K.S. Writing original draft: L.Fa., H.As., J.Be., G.C.T., D.F.E., P.K., A.M.D. Writing review and editing: D.R.B., J.Al., P.So., A.Le., V.N.K., J.D.E., S.L.E., A.C.A., J.Si. Visualization: L.Fa., H.As., J.Be., C.Tu. Supervision: A.C.A., G.C.T., J.Si., D.F.E., P.K., A.M.D. Funding acquisition: L.Fa., P.D.P.P., J.C.C., M.G.C., M.K.S., R.L.M., V.N.K., J.D.E., S.L.E., A.C.A., G.C.T., J.Si., D.F.E., P.K., A.M.D. All authors read and approved the final version of the manuscript.

COMPETING INTERESTS STATEMENT

The authors declare no competing interests.

MATERIALS & CORRESPONDENCE

Further information and requests for resources should be directed to and will be fulfilled by Manjeet Bolla (bcac@medschl.cam.ac.uk)

REFERENCES

1. Milne, R.L. *et al.* Identification of ten variants associated with risk of estrogen-receptor-negative breast cancer. *Nat Genet* **49**, 1767-1778 (2017).
2. Michailidou, K. *et al.* Association analysis identifies 65 new breast cancer risk loci. *Nature* **551**, 92-94 (2017).
3. Ghousaini, M. *et al.* Evidence that breast cancer risk at the 2q35 locus is mediated through IGFBP5 regulation. *Nat Commun* **4**, 4999 (2014).
4. Wyszynski, A. *et al.* An intergenic risk locus containing an enhancer deletion in 2q35 modulates breast cancer risk by deregulating IGFBP5 expression. *Hum Mol Genet* **25**, 3863-3876 (2016).
5. Guo, X. *et al.* Fine-scale mapping of the 4q24 locus identifies two independent loci associated with breast cancer risk. *Cancer Epidemiol Biomarkers Prev* **24**, 1680-91 (2015).
6. Glubb, D.M. *et al.* Fine-scale mapping of the 5q11.2 breast cancer locus reveals at least three independent risk variants regulating MAP3K1. *Am J Hum Genet* **96**, 5-20 (2015).
7. Dunning, A.M. *et al.* Breast cancer risk variants at 6q25 display different phenotype associations and regulate ESR1, RMND1 and CCDC170. *Nat Genet* **48**, 374-86 (2016).
8. Shi, J. *et al.* Fine-scale mapping of 8q24 locus identifies multiple independent risk variants for breast cancer. *Int J Cancer* **139**, 1303-1317 (2016).

9. Orr, N. *et al.* Fine-mapping identifies two additional breast cancer susceptibility loci at 9q31.2. *Hum Mol Genet* **24**, 2966-84 (2015).
10. Darabi, H. *et al.* Polymorphisms in a Putative Enhancer at the 10q21.2 Breast Cancer Risk Locus Regulate NRBF2 Expression. *Am J Hum Genet* **97**, 22-34 (2015).
11. Darabi, H. *et al.* Fine scale mapping of the 17q22 breast cancer locus using dense SNPs, genotyped within the Collaborative Oncological Gene-Environment Study (COGs). *Sci Rep* **6**, 32512 (2016).
12. Meyer, K.B. *et al.* Fine-scale mapping of the FGFR2 breast cancer risk locus: putative functional variants differentially bind FOXA1 and E2F1. *Am J Hum Genet* **93**, 1046-60 (2013).
13. Betts, J.A. *et al.* Long noncoding RNAs CUPID1 and CUPID2 mediate breast cancer risk at 11q13 by modulating the response to dna damage. *Am J Hum Genet* **101**, 255-266 (2017).
14. French, J.D. *et al.* Functional variants at the 11q13 risk locus for breast cancer regulate cyclin D1 expression through long-range enhancers. *Am J Hum Genet* **92**, 489-503 (2013).
15. Ghousaini, M. *et al.* Evidence that the 5p12 variant rs10941679 Confers susceptibility to estrogen-receptor-positive breast cancer through FGF10 and MRPS30 regulation. *Am J Hum Genet* **99**, 903-911 (2016).
16. Horne, H.N. *et al.* Fine-mapping of the 1p11.2 Breast cancer susceptibility locus. *PLoS One* **11**, e0160316 (2016).
17. Zeng, C. *et al.* Identification of independent association signals and putative functional variants for breast cancer risk through fine-scale mapping of the 12p11 locus. *Breast Cancer Res* **18**, 64 (2016).
18. Lin, W.Y. *et al.* Identification and characterization of novel associations in the CASP8/ALS2CR12 region on chromosome 2 with breast cancer risk. *Hum Mol Genet* **24**, 285-98 (2015).

19. Bojesen, S.E. *et al.* Multiple independent variants at the TERT locus are associated with telomere length and risks of breast and ovarian cancer. *Nat Genet* **45**, 371-84, 384e1-2 (2013).
20. Lawrenson, K. *et al.* Functional mechanisms underlying pleiotropic risk alleles at the 19p13.1 breast-ovarian cancer susceptibility locus. *Nat Commun* **7**, 12675 (2016).
21. Amos, C.I. *et al.* The OncoArray Consortium: A Network for Understanding the Genetic Architecture of Common Cancers. *Cancer Epidemiol Biomarkers Prev* **26**, 126-135 (2017).
22. Michailidou, K. *et al.* Large-scale genotyping identifies 41 new loci associated with breast cancer risk. *Nat Genet* **45**, 353-61, 361e1-2 (2013).
23. Michailidou, K. *et al.* Genome-wide association analysis of more than 120,000 individuals identifies 15 new susceptibility loci for breast cancer. *Nature Genetics* **47**, 373-U127 (2015).
24. Udler, M.S., Tyrer, J. & Easton, D.F. Evaluating the power to discriminate between highly correlated SNPs in genetic association studies. *Genet Epidemiol* **34**, 463-8 (2010).
25. Mavaddat, N., Antoniou, A.C., Easton, D.F. & Garcia-Closas, M. Genetic susceptibility to breast cancer. *Mol Oncol* **4**, 174-91 (2010).
26. Lakhani, S.R. *et al.* Prediction of BRCA1 status in patients with breast cancer using estrogen receptor and basal phenotype. *Clin Cancer Res* **11**, 5175-80 (2005).
27. Taberlay, P.C., Statham, A.L., Kelly, T.K., Clark, S.J. & Jones, P.A. Reconfiguration of nucleosome-depleted regions at distal regulatory elements accompanies DNA methylation of enhancers and insulators in cancer. *Genome Res* **24**, 1421-32 (2014).
28. Hnisz, D. *et al.* Super-enhancers in the control of cell identity and disease. *Cell* **155**, 934-47 (2013).
29. Farh, K.K. *et al.* Genetic and epigenetic fine mapping of causal autoimmune disease variants. *Nature* **518**, 337-43 (2015).

30. Cowper-Salari, R. *et al.* Breast cancer risk-associated SNPs modulate the affinity of chromatin for FOXA1 and alter gene expression. *Nat Genet* **44**, 1191-8 (2012).
31. Kichaev, G. *et al.* Integrating functional data to prioritize causal variants in statistical fine-mapping studies. *PLoS Genet* **10**, e1004722 (2014).
32. Quiroz-Zarate, A. *et al.* Expression Quantitative Trait loci (QTL) in tumor adjacent normal breast tissue and breast tumor tissue. *PLoS One* **12**, e0170181 (2017).
33. Cancer Genome Atlas Research, N. *et al.* The Cancer Genome Atlas Pan-Cancer analysis project. *Nat Genet* **45**, 1113-20 (2013).
34. Curtis, C. *et al.* The genomic and transcriptomic architecture of 2,000 breast tumours reveals novel subgroups. *Nature* **486**, 346-52 (2012).
35. Ciriello, G. *et al.* Comprehensive Molecular Portraits of Invasive Lobular Breast Cancer. *Cell* **163**, 506-19 (2015).
36. Nik-Zainal, S. *et al.* Landscape of somatic mutations in 560 breast cancer whole-genome sequences. *Nature* **534**, 47-54 (2016).
37. Pereira, B. *et al.* The somatic mutation profiles of 2,433 breast cancers refines their genomic and transcriptomic landscapes. *Nat Commun* **7**, 11479 (2016).
38. Cancer Genome Atlas, N. Comprehensive molecular portraits of human breast tumours. *Nature* **490**, 61-70 (2012).
39. Bailey, M.H. *et al.* Comprehensive Characterization of Cancer Driver Genes and Mutations. *Cell* **173**, 371-385 e18 (2018).
40. Lambert, S.A. *et al.* The Human Transcription Factors. *Cell* **172**, 650-665 (2018).

41. Artero-Castro, A. *et al.* Disruption of the ribosomal P complex leads to stress-induced autophagy. *Autophagy* **11**, 1499-519 (2015).
42. Wang, X.Y. *et al.* Musashi1 modulates mammary progenitor cell expansion through proliferin-mediated activation of the Wnt and Notch pathways. *Mol Cell Biol* **28**, 3589-99 (2008).
43. Vijayan, D., Young, A., Teng, M.W.L. & Smyth, M.J. Targeting immunosuppressive adenosine in cancer. *Nat Rev Cancer* **17**, 709-724 (2017).
44. Takebe, N. *et al.* Targeting Notch, Hedgehog, and Wnt pathways in cancer stem cells: clinical update. *Nat Rev Clin Oncol* **12**, 445-64 (2015).
45. Thorpe, L.M., Yuzugullu, H. & Zhao, J.J. PI3K in cancer: divergent roles of isoforms, modes of activation and therapeutic targeting. *Nat Rev Cancer* **15**, 7-24 (2015).
46. Nusse, R. & Clevers, H. Wnt/beta-Catenin Signaling, Disease, and Emerging Therapeutic Modalities. *Cell* **169**, 985-999 (2017).
47. Massague, J. TGFbeta signalling in context. *Nat Rev Mol Cell Biol* **13**, 616-30 (2012).
48. Meeks, H.D. *et al.* BRCA2 polymorphic stop codon K3326X and the Risk of breast, prostate, and ovarian cancers. *J Natl Cancer Inst* **108**(2016).
49. CHEK2 Breast Cancer Case-Control Consortium. CHEK2*1100delC and susceptibility to breast cancer: a collaborative analysis involving 10,860 breast cancer cases and 9,065 controls from 10 studies. *Am J Hum Genet* **74**, 1175-82 (2004).
50. Schmidt, M.K. *et al.* Age- and Tumor Subtype-Specific Breast Cancer Risk Estimates for CHEK2*1100delC Carriers. *J Clin Oncol* **34**, 2750-60 (2016).
51. Kilpivaara, O. *et al.* CHEK2 variant I157T may be associated with increased breast cancer risk. *Int J Cancer* **111**, 543-7 (2004).

52. Muranen, T.A. *et al.* Patient survival and tumor characteristics associated with CHEK2:p.I157T - findings from the Breast Cancer Association Consortium. *Breast Cancer Res* **18**, 98 (2016).
53. Killedar, A. *et al.* A Common Cancer Risk-Associated Allele in the hTERT Locus Encodes a Dominant Negative Inhibitor of Telomerase. *PLoS Genet* **11**, e1005286 (2015).
54. De Blasio, A. *et al.* Unusual roles of caspase-8 in triple-negative breast cancer cell line MDA-MB-231. *Int J Oncol* **48**, 2339-48 (2016).
55. Haupt, S. *et al.* Targeting Mdmx to treat breast cancers with wild-type p53. *Cell Death Dis* **6**, e1821 (2015).
56. Pandya, P.H., Murray, M.E., Pollok, K.E. & Renbarger, J.L. The Immune System in Cancer Pathogenesis: Potential Therapeutic Approaches. *J Immunol Res* **2016**, 4273943 (2016).
57. Gionet, N., Jansson, D., Mader, S. & Pratt, M.A. NF-kappaB and estrogen receptor alpha interactions: Differential function in estrogen receptor-negative and -positive hormone-independent breast cancer cells. *J Cell Biochem* **107**, 448-59 (2009).
58. Fleischer, T. *et al.* DNA methylation at enhancers identifies distinct breast cancer lineages. *Nat Commun* **8**, 1379 (2017).
59. Couch, F.J. *et al.* Genome-wide association study in BRCA1 mutation carriers identifies novel loci associated with breast and ovarian cancer risk. *PLoS Genet* **9**, e1003212 (2013).
60. Gaudet, M.M. *et al.* Identification of a BRCA2-specific modifier locus at 6p24 related to breast cancer risk. *PLoS Genet* **9**, e1003173 (2013).
61. Marchini, J., Howie, B., Myers, S., McVean, G. & Donnelly, P. A new multipoint method for genome-wide association studies by imputation of genotypes. *Nat Genet* **39**, 906-13 (2007).

62. Benjamini, Y. & Hochberg, Y. Controlling the False Discovery Rate - a Practical and Powerful Approach to Multiple Testing. *Journal of the Royal Statistical Society Series B-Methodological* **57**, 289-300 (1995).
63. Liu, J.Z. *et al.* Meta-analysis and imputation refines the association of 15q25 with smoking quantity. *Nat Genet* **42**, 436-40 (2010).
64. Antoniou, A.C. *et al.* RAD51 135G-->C modifies breast cancer risk among BRCA2 mutation carriers: results from a combined analysis of 19 studies. *Am J Hum Genet* **81**, 1186-200 (2007).
65. Barnes, D.R. *et al.* Evaluation of association methods for analysing modifiers of disease risk in carriers of high-risk mutations. *Genet Epidemiol* **36**, 274-91 (2012).
66. Willer, C.J., Li, Y. & Abecasis, G.R. METAL: fast and efficient meta-analysis of genomewide association scans. *Bioinformatics* **26**, 2190-1 (2010).
67. Hunter, D.J. *et al.* A genome-wide association study identifies alleles in FGFR2 associated with risk of sporadic postmenopausal breast cancer. *Nat Genet* **39**, 870-4 (2007).
68. Baran, Y. *et al.* Fast and accurate inference of local ancestry in Latino populations. *Bioinformatics* **28**, 1359-67 (2012).
69. Howie, B., Fuchsberger, C., Stephens, M., Marchini, J. & Abecasis, G.R. Fast and accurate genotype imputation in genome-wide association studies through pre-phasing. *Nat Genet* **44**, 955-9 (2012).
70. Genomes Project, C. *et al.* An integrated map of genetic variation from 1,092 human genomes. *Nature* **491**, 56-65 (2012).
71. Li, B. & Dewey, C.N. RSEM: accurate transcript quantification from RNA-Seq data with or without a reference genome. *BMC Bioinformatics* **12**, 323 (2011).

72. Mermel, C.H. *et al.* GISTIC2.0 facilitates sensitive and confident localization of the targets of focal somatic copy-number alteration in human cancers. *Genome Biol* **12**, R41 (2011).
73. Li, Q. *et al.* Integrative eQTL-based analyses reveal the biology of breast cancer risk loci. *Cell* **152**, 633-41 (2013).
74. Shabalin, A.A. Matrix eQTL: ultra fast eQTL analysis via large matrix operations. *Bioinformatics* **28**, 1353-8 (2012).
75. ENCODE Project Consortium. An integrated encyclopedia of DNA elements in the human genome. *Nature* **489**, 57-74 (2012).
76. Sloan, C.A. *et al.* ENCODE data at the ENCODE portal. *Nucleic Acids Res* **44**, D726-32 (2016).
77. Roadmap Epigenomics, C. *et al.* Integrative analysis of 111 reference human epigenomes. *Nature* **518**, 317-30 (2015).
78. Stunnenberg, H.G., International Human Epigenome, C. & Hirst, M. The International Human Epigenome Consortium: A Blueprint for Scientific Collaboration and Discovery. *Cell* **167**, 1897 (2016).
79. Pellacani, D. *et al.* Analysis of Normal Human Mammary Epigenomes Reveals Cell-Specific Active Enhancer States and Associated Transcription Factor Networks. *Cell Rep* **17**, 2060-2074 (2016).
80. Cheneby, J., Gheorghe, M., Artufel, M., Mathelier, A. & Ballester, B. ReMap 2018: an updated atlas of regulatory regions from an integrative analysis of DNA-binding ChIP-seq experiments. *Nucleic Acids Res* **46**, D267-D275 (2018).
81. Pruitt, K.D. *et al.* RefSeq: an update on mammalian reference sequences. *Nucleic Acids Res* **42**, D756-63 (2014).

82. Harrow, J. *et al.* GENCODE: the reference human genome annotation for The ENCODE Project. *Genome Res* **22**, 1760-74 (2012).
83. Wang, J. *et al.* Sequence features and chromatin structure around the genomic regions bound by 119 human transcription factors. *Genome Res* **22**, 1798-812 (2012).
84. Mathelier, A. *et al.* JASPAR 2016: a major expansion and update of the open-access database of transcription factor binding profiles. *Nucleic Acids Res* **44**, D110-5 (2016).
85. Tan, G. & Lenhard, B. TFBSTools: an R/bioconductor package for transcription factor binding site analysis. *Bioinformatics* **32**, 1555-6 (2016).
86. Grant, C.E., Bailey, T.L. & Noble, W.S. FIMO: scanning for occurrences of a given motif. *Bioinformatics* **27**, 1017-8 (2011).
87. Grassi, E., Zapparoli, E., Molineris, I. & Provero, P. Total Binding Affinity Profiles of Regulatory Regions Predict Transcription Factor Binding and Gene Expression in Human Cells. *PLoS One* **10**, e0143627 (2015).
88. Quinlan, A.R. & Hall, I.M. BEDTools: a flexible suite of utilities for comparing genomic features. *Bioinformatics* **26**, 841-2 (2010).
89. McLeay, R.C. & Bailey, T.L. Motif Enrichment Analysis: a unified framework and an evaluation on ChIP data. *BMC Bioinformatics* **11**, 165 (2010).
90. Kichaev, G. *et al.* Improved methods for multi-trait fine mapping of pleiotropic risk loci. *Bioinformatics* **33**, 248-255 (2017).
91. McLaren, W. *et al.* The Ensembl Variant Effect Predictor. *Genome Biol* **17**, 122 (2016).
92. Adzhubei, I.A. *et al.* A method and server for predicting damaging missense mutations. *Nat Methods* **7**, 248-9 (2010).

93. Kumar, P., Henikoff, S. & Ng, P.C. Predicting the effects of coding non-synonymous variants on protein function using the SIFT algorithm. *Nat Protoc* **4**, 1073-81 (2009).
94. Stone, E.A. & Sidow, A. Physicochemical constraint violation by missense substitutions mediates impairment of protein function and disease severity. *Genome Res* **15**, 978-86 (2005).
95. Yeo, G. & Burge, C.B. Maximum entropy modeling of short sequence motifs with applications to RNA splicing signals. *J Comput Biol* **11**, 377-94 (2004).
96. Desmet, F.O. *et al.* Human Splicing Finder: an online bioinformatics tool to predict splicing signals. *Nucleic Acids Res* **37**, e67 (2009).
97. Beesley, J. *et al.* Chromatin interactome mapping at 139 independent breast cancer risk signals. *Submitted*.
98. Fullwood, M.J. *et al.* An oestrogen-receptor-alpha-bound human chromatin interactome. *Nature* **462**, 58-64 (2009).
99. Corradin, O. *et al.* Combinatorial effects of multiple enhancer variants in linkage disequilibrium dictate levels of gene expression to confer susceptibility to common traits. *Genome Res* **24**, 1-13 (2014).
100. Andersson, R. *et al.* An atlas of active enhancers across human cell types and tissues. *Nature* **507**, 455-461 (2014).
101. Moradi Marjaneh, M. *et al.* High-throughput allelic expression imbalance analyses identify 14 candidate breast cancer risk genes. *Submitted*.
102. Dixon, J.R. *et al.* Integrative detection and analysis of structural variation in cancer genomes. *Nat Genet* **50**, 1388-1398 (2018).

103. Merico, D., Isserlin, R. & Bader, G.D. Visualizing gene-set enrichment results using the Cytoscape plug-in enrichment map. *Methods Mol Biol* **781**, 257-77 (2011).
104. Vastrik, I. *et al.* Reactome: a knowledge base of biologic pathways and processes. *Genome Biol* **8**, R39 (2007).
105. Schaefer, C.F. *et al.* PID: the Pathway Interaction Database. *Nucleic Acids Res* **37**, D674-9 (2009).
106. Ashburner, M. *et al.* Gene ontology: tool for the unification of biology. The Gene Ontology Consortium. *Nat Genet* **25**, 25-9 (2000).
107. Romero, P. *et al.* Computational prediction of human metabolic pathways from the complete human genome. *Genome Biol* **6**, R2 (2005).
108. Subramanian, A. *et al.* Gene set enrichment analysis: a knowledge-based approach for interpreting genome-wide expression profiles. *Proc Natl Acad Sci U S A* **102**, 15545-50 (2005).
109. Kandasamy, K. *et al.* NetPath: a public resource of curated signal transduction pathways. *Genome Biol* **11**, R3 (2010).
110. Thomas, P.D. *et al.* PANTHER: a library of protein families and subfamilies indexed by function. *Genome Res* **13**, 2129-41 (2003).
111. Herwig, R., Hardt, C., Lienhard, M. & Kamburov, A. Analyzing and interpreting genome data at the network level with ConsensusPathDB. *Nat Protoc* **11**, 1889-907 (2016).

Table 1. Signals with single CCVs and variants with PP > 80%

| Fine-mapping region ^a | Variant ^b | Ref/Alt ^c | EAF ^d | PP ^e | Model ^f | Signal ^g | N CCV ^h | ER-negative | | ER-positive | | P-value ⁱ | FP ^j | Predicted target gene(s) ^k | Confidence ^l |
|----------------------------------|----------------------|----------------------|------------------|-----------------|--------------------|---------------------|--------------------|-----------------|-------------|-----------------|-------------|------------------------|-----------------|---|-------------------------|
| | | | | | | | | OR ⁱ | (95%CI) | OR ⁱ | (95%CI) | | | | |
| chr1:120723447-121780613 | rs11249433 | A/G | 0.42 | 0.57 | ERALL | Signal 1 | 1 | 1.02 | (0.99-1.04) | 1.13 | (1.11-1.15) | 8.11x10 ⁻⁶⁰ | na | na | |
| chr1:200937832-201937832 | rs35383942 | C/T | 0.06 | 0.96 | ERALL | Signal 1 | 2 | 1.10 | (1.05-1.16) | 1.09 | (1.06-1.13) | 1.14x10 ⁻⁷ | D | <i>TNNI1</i> | Level 1 |
| chr2:201681247-202681247 | rs3769821 | C/T | 0.66 | 0.40 | ERALL | Signal 1 | 1 | 0.94 | (0.92-0.97) | 0.95 | (0.93-0.96) | 1.46x10 ⁻¹² | D | <i>ALS2CR11</i> , <i>ALS2CR12</i> , <i>CASP8^m</i> , <i>MPP4</i> , <i>NIF3L1</i> , <i>STRADB</i> , <i>TMEM237</i> | Level 2 |
| chr2:217405832-218796508 | rs4442975 | G/T | 0.48 | 0.84 | ERALL | Signal 1 | 1 | 0.94 | (0.92-0.97) | 0.86 | (0.85-0.87) | 2.50x10 ⁻⁹⁰ | D | <i>IGFBP5^m</i> | Level 1 |
| chr4:105569013-106856761 | esv3601665 | -/Alu | 0.07 | 0.95 | ERPOS | | | 1.01 | (0.95-1.08) | 1.10 | (1.06-1.14) | 3.27x10 ⁻⁶ | D | <i>ARHGEF38</i> , <i>AC004066.3</i> | Level 1 |
| chr5:779790-1797488 | rs10069690 | C/T | 0.27 | 0.58 | ERNEG | Signal 1 | 1 | 1.18 | (1.15-1.21) | 1.03 | (1.01-1.05) | 1.20x10 ⁻³⁴ | D | <i>CLPTM1L</i> , <i>TERT^m</i> | Level 1 |
| chr5:44013304-45206498 | rs10941679 | A/G | 0.26 | 0.00 | ERPOS | Signal 1 | 1 | 1.04 | (1.02-1.07) | 1.17 | (1.15-1.19) | 1.50x10 ⁻⁷⁷ | D | <i>MRPS30</i> | Level 2 |
| | rs5867671 | A/- | 0.77 | 0.01 | ERPOS | Signal 2 | 1 | 0.91 | (0.89-0.94) | 0.99 | (0.97-1.01) | 2.25x10 ⁻⁹ | na | na | |
| chr5:44013304-45206498 | rs190443933 | T/C | 0.01 | 0.00 | ERALL | Signal 4 | 1 | 1.30 | (1.14-1.48) | 1.26 | (1.16-1.37) | 2.32x10 ⁻⁸ | na | na | |
| chr5:55531884-56587883 | rs984113 | G/C | 0.61 | 0.81 | ERPOS | Signal 2 | 1 | 0.96 | (0.93-0.98) | 0.96 | (0.94-0.97) | 3.51x10 ⁻⁸ | D | <i>MAP3K1^m</i> | Level 1 |
| | rs889310 | C/T | 0.56 | 0.84 | ERPOS | (Signal 6) | 15 | 1.03 | (1.00-1.05) | 1.05 | (1.03-1.06) | 1.75x10 ⁻⁷ | D | <i>MAP3K1^m</i> | Level 1 |
| chr6:15899557-16899557 | rs3819405 | C/T | 0.32 | 0.96 | ERALL | Signal 1 | 1 | 0.97 | (0.95-1.00) | 0.95 | (0.94-0.97) | 1.14x10 ⁻⁷ | D | <i>ATXN1</i> , <i>RP1-151F17.1</i> , <i>RP1-151F17.2</i> | Level 2 |
| chr6:151418856-152937016 | rs12173562 | C/T | 0.08 | 0.10 | ERNEG | Signal 1 | 1 | 1.30 | (1.25-1.36) | 1.14 | (1.11-1.18) | 3.98x10 ⁻⁴⁰ | D | <i>ESR1^m</i> | Level 1 |
| | rs34133739 | -/C | 0.53 | 0.25 | ERALL | Signal 2 | 1 | 1.11 | (1.09-1.14) | 1.05 | (1.04-1.07) | 2.36x10 ⁻²² | D | <i>ESR1^m</i> , <i>SYNE1</i> | Level 2 |
| | rs851984 | G/A | 0.40 | 0.73 | ERALL | Signal 3 | 1 | 1.07 | (1.04-1.09) | 1.05 | (1.04-1.07) | 3.69x10 ⁻¹³ | D | <i>ESR1^m</i> | Level 1 |
| chr7:130167121-131167121 | rs68056147 | G/A | 0.30 | 0.84 | ERALL | | | 1.04 | (1.01-1.07) | 1.05 | (1.03-1.06) | 3.07x10 ⁻⁷ | D | <i>MKLN1</i> | Level 2 |
| chr8:127424659-130041931 | rs35961416 | -/A | 0.41 | 0.68 | ERALL | Signal 3 | 1 | 0.97 | (0.94-0.99) | 0.95 | (0.93-0.96) | 9.97x10 ⁻¹¹ | D | <i>CASC11</i> , <i>MYC^m</i> | Level 2 |
| chr9:21247803-22624477 | rs539723051 | AAAA/- | 0.33 | 0.43 | ERALL | Signal 1 | 1 | 1.08 | (1.05-1.11) | 1.06 | (1.04-1.08) | 1.81x10 ⁻¹⁵ | na | na | |

| | | | | | | | | | | | | | | | |
|---------------------------|-------------|------|------|------|-------|----------|---|------|-------------|------|-------------|-------------------------|------|---|---------|
| chr9:109803808-111395353 | rs10816625 | A/G | 0.07 | 0.95 | ERPOS | Signal 3 | 1 | 1.06 | (1.01-1.11) | 1.13 | (1.10-1.16) | 3.62x10 ⁻¹⁵ | D | <i>KLF4^m</i> | Level 2 |
| | rs13294895 | C/T | 0.18 | 0.93 | ERPOS | Signal 4 | 1 | 1.01 | (0.98-1.05) | 1.09 | (1.07-1.11) | 4.00x10 ⁻¹⁷ | D | <i>KLF4^m</i> | Level 1 |
| chr9:109803808-111395353 | rs60037937 | AA/- | 0.22 | 0.68 | ERPOS | Signal 2 | 1 | 1.02 | (0.99-1.06) | 1.11 | (1.09-1.13) | 3.17x10 ⁻²⁶ | D | <i>KLF4^m, RAD23B</i> | Level 2 |
| chr10:63758684-65063702 | rs10995201 | A/G | 0.15 | 0.31 | ERALL | Signal 1 | 1 | 0.91 | (0.88-0.94) | 0.87 | (0.85-0.89) | 1.40x10 ⁻³⁷ | na | na | |
| chr10:122593901-123849324 | rs45631563 | A/T | 0.04 | 0.93 | ERPOS | Signal 3 | 1 | 0.97 | (0.92-1.03) | 0.76 | (0.73-0.79) | 4.84x10 ⁻⁴⁴ | C | <i>FGFR2^m</i> | Level 1 |
| chr10:122593901-123849324 | rs35054928 | C/- | 0.56 | 0.60 | ERALL | Signal 1 | 1 | 0.96 | (0.94-0.98) | 0.74 | (0.73-0.76) | 6.55x10 ⁻³⁴² | D | <i>FGFR2^m</i> | Level 1 |
| | rs45631563 | A/T | 0.04 | 0.93 | ERPOS | Signal 3 | 1 | 0.97 | (0.92-1.03) | 0.76 | (0.73-0.79) | 4.84x10 ⁻⁴⁴ | C | <i>FGFR2^m</i> | Level 1 |
| | rs7899765 | T/C | 0.06 | 0.02 | ERALL | Signal 5 | 1 | 1.01 | (0.97-1.06) | 0.87 | (0.84-0.90) | 2.21x10 ⁻¹⁸ | D | <i>FGFR2^m</i> | Level 1 |
| chr11:68831418-69879161 | rs78540526 | C/T | 0.09 | 0.91 | ERPOS | Signal 1 | 1 | 1.01 | (0.97-1.06) | 1.40 | (1.36-1.44) | 2.77x10 ⁻¹⁴⁵ | D | <i>CCND1^m, MYEOV</i> | Level 1 |
| chr12:27639846-29034415 | rs7297051 | C/T | 0.23 | 0.23 | ERALL | Signal 1 | 1 | 0.87 | (0.85-0.90) | 0.89 | (0.88-0.91) | 3.12x10 ⁻⁴³ | D | <i>CCDC91^m, PTHLH^m, RP11-967K21.1</i> | Level 2 |
| chr12:115336522-116336522 | rs35422 | G/A | 0.57 | 0.58 | ERPOS | Signal 2 | 1 | 0.98 | (0.96-1.01) | 1.05 | (1.03-1.07) | 4.85x10 ⁻¹⁰ | D | <i>TBX3</i> | Level 1 |
| chr14:91341069-92368623 | rs7153397 | C/T | 0.70 | 0.81 | ERPOS | Signal 1 | 3 | 1.01 | (0.99-1.04) | 1.06 | (1.04-1.08) | 3.25x10 ⁻¹¹ | D,C | <i>CCDC88C, CTD-2547L24.4, GPR68, RP11-73M18.7, RP11-895M11.3</i> | Level 2 |
| chr16:52038825-53038825 | rs4784227 | C/T | 0.27 | 0.95 | ERPOS | Signal 1 | 1 | 1.15 | (1.12-1.18) | 1.26 | (1.24-1.28) | 4.63x10 ⁻¹⁶⁰ | D | <i>TOX3^m</i> | Level 1 |
| chr18:23832476-25075396 | rs180952292 | T/C | 0.01 | 0.01 | ERNEG | Signal 4 | 1 | 1.24 | (1.12-1.37) | 0.98 | (0.92-1.05) | 2.07x10 ⁻⁵ | na | na | |
| chr18:41899590-42899590 | rs9952980 | T/C | 0.34 | 0.95 | ERALL | Signal 2 | 3 | 0.97 | (0.94-0.99) | 0.95 | (0.93-0.96) | 7.43x10 ⁻¹² | D | <i>SETBP1</i> | Level 2 |
| chr20:5448227-6448227 | rs16991615 | G/A | 0.07 | 0.97 | ERALL | Signal 1 | 1 | 1.09 | (1.04-1.15) | 1.07 | (1.04-1.11) | 7.89x10 ⁻⁷ | D, C | <i>GPCPD1, MCM8</i> | Level 2 |
| chr22:45783297-46783297 | rs184070480 | C/T | 0.01 | 0.00 | ERALL | Signal 2 | 1 | 1.40 | (1.20-1.64) | 1.01 | (0.91-1.12) | 5.02x10 ⁻⁵ | D | <i>ATXN10, WNT7B</i> | Level 2 |

^a GRCh37/hg19, bp

^b Current reference ID

^c Reference (Ref) versus Alternative (Alt) Allele

^d Effect allele (Alt allele) frequency in OncoArray

^e PP: Posterior probability. Largest posterior probability in all evaluated models

^f Model where the variant reaches the largest posterior probability

^g Signal where the variant is included. Between brackets moderate confidence signals.

^h Number of CCVs in the signal

ⁱ Multinomial regression summary statistics. Single variant analysis

^j D: Distal regulation, P: proximal regulation, C: coding; na: prediction non available

^k Predicted target genes with the largest confidence level for each variant. Between brackets, largest confidence level. na: prediction non available

^l INQUISIT level of confidence

^m Target genes with functional follow up

Table 2. Regions in which target genes are predicted with high confidence

| Fine-mapping region ^a | Signal / PP >30% ^b | N Variants ^c | Distal ^d | Promoter ^e | Coding ^f |
|----------------------------------|----------------------------------|----------------------------|---|-----------------------|---------------------|
| chr1:10043820-11066215 | Signal 1 | 19 | <i>PEX14</i> | | |
| chr1:18307339-19307339 | Signal 1 | 12 | | <i>KLHDC7A</i> | |
| | PP > 30% | 1 | | <i>KLHDC7A</i> | |
| chr1:46100917-47100917 | Signal 1 | 11 | <i>LRRC41, PIK3R3</i> | | |
| | PP > 30% | 2 | <i>MAST2, POMGNT1</i> | | |
| chr1:113948389-114948389 | Signal 1 | 12 | <i>RSBN1</i> | | |
| chr1:145144984-146144984 | Signal 1 | 35 | <i>NUDT17, PDZK1, RNF115</i> | | |
| | Signal 2 | 5 | <i>PIAS3</i> | | |
| chr1:154648781-155648781 | Signal 1 | 16 | <i>EFNA1, FAM189B, GBA, MTX1, MUC1, RP11-263K19.4, SLC50A1, THBS3, TRIM46</i> | | |
| chr1:200937832-201937832 | Signal 1 | 2 | <i>TNNI1</i> | | |
| | PP > 30% | 2 | <i>TNNI1</i> | | |
| chr1:203301249-204301249 | Signal 1 | 56 | <i>SOX13</i> | | |
| chr1:204018842-205018842 | Signal 1 | 6 | <i>LRRN2, MDM4, PIK3C2B, PPP1R15B</i> | <i>MDM4</i> | |
| chr1:241523898-242534263 | Signal 1 | 2 | | | <i>EXO1</i> |
| | PP > 30% | 2 | | | <i>EXO1</i> |
| chr2:18815791-19820803 | Signal 1 | 17 | <i>OSR1</i> | | |
| chr2:24687599-25687599 | Signal 1 | 92 | <i>ADCY3, DNMT3A</i> | | <i>DNMT3A</i> |
| chr2:28670676-29670676 | Signal 1 | 81 | <i>PPP1CB, TRMT61B</i> | | |
| chr2:120745122-121746568 | Signal 3 | 3 | <i>INHBB</i> | | |
| | Signal 4 | 6 | <i>INHBB</i> | | |
| | PP > 30% | 3 | <i>INHBB</i> | | |
| chr2:171876221-173472971 | Signal 2 | 35 | <i>DYNC1I2</i> | | |
| | PP > 30% | 2 | <i>DYNC1I2</i> | | |
| chr2:201681247-202681247 | Signal 2 | 8 | <i>CFLAR</i> | | |
| | CIMBA | 154 | <i>CASP8, CFLAR, NIF3L1, PPIL3</i> | <i>CASP8</i> | |
| chr2:217405832-218796508 | PP > 30% | 6 | <i>IGFBP5</i> | | |
| chr3:30175880-31175880 | Signal 1 | 23 | | | <i>TGFBR2</i> |
| chr3:46366866-47381488 | CIMBA | 16 | <i>CCDC12, NBEAL2</i> | | |
| chr3:63441697-64467900 | Signal 1 | 94 | <i>ATXN7, PSMD6, PSMD6-AS2, THOC7</i> | | <i>ATXN7</i> |
| chr3:99223580-100223580 | Signal 1 | 92 | <i>CMSS1, FILIP1L, TBC1D23</i> | | |
| chr3:140612859-141612859 | Signal 1 | 24 | <i>ZBTB38</i> | | |
| chr3:171785237-172785237 | CIMBA | 36 | <i>TNFSF10</i> | | |
| chr4:38312876-39312876 | Signal 1 | 24 | | | <i>TLR1</i> |
| chr4:83870124-84870124 | Signal 1 | 84 | <i>MRPS18C</i> | <i>MRPS18C</i> | |
| chr4:105569013-106856761 | Signal 1 | 21 | <i>TET2</i> | | <i>TET2</i> |
| | PP > 30% | 1 | <i>AC004066.3, ARHGEF38</i> | | |
| chr5:779790-1797488 | Signal 3 | 23 | <i>CLPTM1L, TERT</i> | | |
| | PP > 30% | 7 | <i>CLPTM1L, TERT</i> | | |
| chr5:55531884-56587883 | Signal 1 | 3 | <i>MAP3K1</i> | | |
| | Signal 3 | 21 | <i>MAP3K1</i> | | <i>MAP3K1</i> |

| | | | | |
|---------------------------|----------|-----|----------------------------------|-----------|
| | Signal 4 | 70 | MAP3K1 | |
| | Signal 5 | 4 | MAP3K1 | |
| | PP > 30% | 5 | MAP3K1 | |
| chr5:90289470-91289470 | Signal 1 | 88 | ARRDC3 | ARRDC3 |
| chr5:131907058-132907058 | Signal 1 | 117 | AFF4, HSPA4, ZCCHC10 | HSPA4 |
| | PP > 30% | 1 | AFF4, HSPA4 | |
| chr5:157730013-158744083 | Signal 1 | 5 | EBF1 | |
| chr5:169091487-170091487 | Signal 1 | 19 | FOXI1 | |
| chr6:13213099-14222523 | Signal 1 | 51 | NOL7, RANBP9, RP1-223E5.4 | |
| chr6:20121238-21121238 | Signal 1 | 52 | CDKAL1 | |
| chr6:28422437-29426220 | Signal 1 | 36 | TRIM27 | |
| chr6:129849119-130849119 | Signal 1 | 43 | | L3MBTL3 |
| chr6:151418856-152937016 | Signal 1 | 1 | ESR1 | |
| | Signal 3 | 1 | ESR1 | |
| | Signal 4 | 6 | C6orf211, CCDC170, ESR1 | |
| | Signal 5 | 173 | | ESR1 |
| | Signal 6 | 22 | CCDC170, ESR1 | ESR1 ESR1 |
| | PP > 30% | 4 | ESR1 | |
| chr7:91130620-92181597 | Signal 1 | 318 | KRIT1 | AKAP9 |
| chr7:101054599-102054599 | Signal 1 | 6 | CUX1 | CUX1 |
| chr8:29009616-30009616 | Signal 1 | 16 | DUSP4 | |
| chr8:101978959-102978959 | Signal 1 | 47 | GRHL2, KB-1562D12.1, KB-1930G5.4 | |
| | PP > 30% | 2 | KB-1930G5.4 | |
| chr8:116709548-117709548 | Signal 1 | 164 | TRPS1 | |
| chr8:124110166-125110166 | Signal 1 | 23 | FBXO32 | |
| | Signal 2 | 6 | FBXO32 | |
| | PP > 30% | 1 | FBXO32, WDYHV1 | |
| chr8:127424659-130041931 | Signal 2 | 44 | MYC | |
| | PP > 30% | 5 | MYC | |
| chr9:109803808-111395353 | Signal 4 | 1 | KLF4 | |
| | PP > 30% | 6 | KLF4 | |
| chr10:8588113-9588113 | Signal 1 | 49 | GATA3 | |
| | PP > 30% | 1 | GATA3 | |
| chr10:21532942-22909392 | Signal 2 | 58 | BMI1, COMMD3 | |
| chr10:80341148-81387721 | Signal 1 | 10 | ZMIZ1 | |
| | Signal 3 | 9 | ZCCHC24 | |
| | PP > 30% | 2 | ZMIZ1 | |
| chr10:114273927-115286154 | Signal 2 | 42 | TCF7L2 | |
| chr10:122593901-123849324 | Signal 1 | 1 | FGFR2 | |
| | Signal 2 | 7 | FGFR2 | |
| | Signal 3 | 1 | | FGFR2 |
| | Signal 4 | 3 | | FGFR2 |
| | Signal 5 | 1 | FGFR2 | |
| | PP > 30% | 6 | FGFR2 | FGFR2 |

| | | | | |
|---------------------------|----------|-----|--|----------------|
| chr11:303017-1303017 | Signal 1 | 19 | <i>CD151, EPS8L2, PDDC1</i> | <i>PIDD1</i> |
| chr11:65043827-66083066 | Signal 1 | 13 | <i>AP5B1, CFL1, OVOL1, RNASEH2C</i> | |
| chr11:68831418-69879161 | Signal 1 | 1 | <i>CCND1, MYEOV</i> | |
| | Signal 2 | 3 | <i>CCND1, MYEOV</i> | |
| | Signal 3 | 20 | <i>CCND1, MYEOV</i> | |
| | PP > 30% | 5 | <i>CCND1, MYEOV</i> | |
| chr11:107845515-108857137 | Signal 1 | 59 | <i>C11orf65, KDELC2</i> | <i>ATM</i> |
| | CIMBA | 8 | | <i>ATM</i> |
| chr12:13913931-14913931 | Signal 1 | 18 | <i>ATF7IP</i> | |
| chr12:27639846-29034415 | Signal 2 | 375 | <i>CCDC91, PTHLH</i> | |
| chr12:95527759-96527759 | Signal 1 | 2 | <i>NTN4</i> | |
| | PP > 30% | 1 | <i>NTN4</i> | |
| chr12:115336522-116336522 | Signal 1 | 7 | <i>TBX3</i> | |
| | Signal 2 | 1 | <i>TBX3</i> | |
| | Signal 3 | 8 | <i>TBX3</i> | |
| | PP > 30% | 7 | <i>TBX3</i> | |
| chr12:120332146-121332146 | Signal 1 | 5 | <i>MSI1, RPLP0</i> | |
| | PP > 30% | 1 | <i>RPLP0</i> | |
| chr13:32468810-33472626 | Signal 1 | 5 | | <i>BRCA2</i> |
| chr14:36632769-37635752 | Signal 1 | 19 | <i>PAX9, SLC25A21</i> | |
| | PP > 30% | 3 | <i>PAX9</i> | |
| chr14:68117194-69534682 | Signal 1 | 8 | <i>ZFP36L1</i> | |
| | Signal 2 | 4 | <i>ZFP36L1</i> | |
| | PP > 30% | 3 | <i>ZFP36L1</i> | |
| chr14:92604072-93616351 | Signal 1 | 34 | | <i>RIN3</i> |
| chr15:91009215-92009215 | Signal 1 | 22 | <i>RCCD1</i> | |
| chr16:3606788-4606788 | Signal 1 | 23 | <i>ADCY9, CREBBP</i> | |
| chr16:52038825-53038825 | Signal 1 | 1 | <i>TOX3</i> | |
| | PP > 30% | 2 | <i>TOX3</i> | |
| chr16:53300954-54355291 | Signal 1 | 6 | <i>CTD-3032H12.2, FTO, IRX3</i> | |
| chr16:54182064-55182064 | Signal 1 | 3 | <i>CRNDE</i> | |
| chr16:80148327-81150805 | Signal 1 | 14 | <i>CDYL2, DYNLRB2, RP11-18F14.4, RP11-525K10.3</i> | |
| | PP > 30% | 1 | <i>DYNLRB2</i> | |
| chr17:77281387-78281725 | Signal 1 | 10 | <i>CCDC40</i> | |
| chr18:23832476-25075396 | Signal 3 | 31 | <i>KCTD1</i> | |
| | PP > 30% | 6 | <i>KCTD1</i> | |
| chr18:41899590-42899590 | Signal 1 | 38 | <i>SETBP1</i> | <i>SETBP1</i> |
| chr19:12658277-14454571 | Signal 1 | 21 | <i>DAND5, GCDH, HOOK2, JUNB, MAST1, PRDX2</i> | |
| chr19:16795023-17894124 | Signal 1 | 16 | <i>ABHD8, MRPL34</i> | |
| | CIMBA | 10 | <i>ABHD8, MRPL34</i> | <i>ANKLE1</i> |
| chr19:18050434-19071141 | Signal 1 | 56 | <i>CRLF1, ELL, FKBP8, GDF15, ISYNA1, KXD1, UBA52</i> | |
| chr19:19048246-20048246 | Signal 1 | 162 | <i>ATP13A1, GATAD2A, LPAR2, MAU2, MEF2B, MEF2BNB, NDUFA13, PBX4, RFXANK, SUGP1</i> | <i>GATAD2A</i> |
| chr19:29777729-30777729 | Signal 1 | 60 | <i>CCNE1</i> | |

| | | | | | | |
|-------------------------|----------|-----|----------------------------------|-------|-------|--|
| chr19:43783447-44786513 | Signal 1 | 10 | KCNN4, PLAUR, SMG9 | | | |
| chr21:16073983-17073983 | Signal 1 | 7 | NRIP1 | | | |
| | PP > 30% | 5 | NRIP1 | | | |
| chr22:28000000-30121477 | Signal 1 | 3 | CHEK2 | | | |
| | Signal 2 | 2 | CHEK2 | | | |
| | Signal 3 | 59 | CHEK2, CTA-292E10.6, EWSR1, XBP1 | CHEK2 | CHEK2 | |
| | PP > 30% | 3 | CHEK2, XBP1 | | | |
| chr22:38068833-39859355 | Signal 1 | 27 | MAFF, PLA2G6, TMEM184B | | | |
| | Signal 3 | 4 | CBX6, NPTXR, SUN2 | | | |
| chr22:40376234-41527870 | Signal 1 | 196 | MKL1, SLC25A17 | | | |
| chr22:41538786-42538786 | Signal 1 | 10 | EP300 | | | |
| chr22:45783297-46783297 | Signal 1 | 34 | WNT7B | | | |

^a GRCh37/hg19, bp

^b Independent signal or set of variants with PP \geq 30%

^c Number of CCV or number of variants with PP \geq 30%

High confidence target genes by ^d distal regulatory, ^e promoter, or ^f coding variants at the signal or at the set of variants with PP \geq 30%